Central place foragers, prey depletion halos, and how behavioral niche partitioning promotes consumer coexistence

Claus Rueffler* and Laurent Lehmann†

Abstract

Many seabirds congregate in large colonies for breeding, a time when they are central place foragers. An influential idea in seabird ecology posits that competition during breeding results in an area of reduced prey availability around colonies, a phenomenon known as *Ashmole's halo*, and that this limits colony size. This idea has gained empirical support, including the finding that species coexisting within a colony might be able to do so by foraging on a single prey species but at different distances. Here, we provide a comprehensive mathematical model for central place foragers exploiting a single prey in a two-dimensional environment, where the prey distribution is the result of intrinsic birth and death, movement in space and mortality due to foraging birds (we also consider a variant tailored toward colonial social insects). Prey mortality is the result of bird predation at different distances according to an ideal free distribution that maximizes prey delivery under flight and search costs. We fully characterize the birds' ideal free distribution and the concomitant prey distribution. Our results show that prey depletion halos around breeding colonies are a robust phenomenon and that the birds' ideal free distribution is sensitive to prey movement. Furthermore, coexistence of several seabird species on a single prey easily emerges through behavioral niche partitioning whenever trait differences between species entail trade-offs between efficiently exploiting a scarce prey close to the colony and a more abundant prey far away. Such behavioral-based coexistence-inducing mechanisms should generalize to other habitat and diet choice scenarios.

*Department of Ecology and Genetics, Animal Ecology, Uppsala University, Sweden; claus.rueffler@ebc.uu.se
†Department of Ecology and Evolution, University of Lausanne, Switzerland; laurent.lehmann@unil.ch

Keywords: Ashmole's halo, seabirds, consumer-resource interactions, ideal free distribution, individual foraging, group foraging, social insects

Significance statement. Large numbers of seabirds, often belonging to different species, breed on small islands and forage in the surrounding sea to provision their offspring. Due to travel costs, these birds are restricted to a limited area around their colony. Using mathematical modelling, we show that such central place foragers produce a zone of prey depletion around islands. In agreement with empirical observations, our model furthermore shows that different bird species can coexist, despite feeding on the same prey species, due to behavioral segregation into different circular zones around the island. Behavioral segregation emerges when individuals chose foraging distances so as to maximize their prey delivery rate and when different species experience different costs while flying to and foraging at different distances.

1 Introduction

Seabird colonies can reach very large numbers (Furness and Monaghan, 1987; Coulson, 2002; Mitchell et al., 2004; Patterson et al., 2022), and various mechanisms have been proposed to explain the limits to colony size. The most influential one is due to Ashmole (1963), who reasoned that during the breeding season seabirds are restricted to an area around their colony because time intervals between visits to the nest cannot be too long and energetic costs for foraging trips cannot be too high if prey is to be delivered at a sufficiently high rate to nestlings. Thus, during breeding, colonial seabirds are *central place foragers*. Ashmole (1963) hypothesized that this area-restricted foraging activity leads to a zone of prey depletion around large colonies, a phenomenon dubbed *Ashmole's halo* (Birt et al., 1987). It is during this breeding phase that population size is regulated through negative density dependence (for reviews see Furness and Monaghan, 1987 and Cairns, 1992).

Over the years, several authors have provided empirical evidence for prey depletion halo's around seabird colonies (Furness and Birkhead, 1984; Birt et al., 1987; Lewis et al., 2001; Forero et al., 2002; Elliott et al., 2009). Most recently, Weber et al. (2021) provided the most convincing evidence to date, based on data collected around Ascension Island, the place where Ashmole did his original research (Ashmole, 1963). A further finding reported by Weber et al. (2021) is

that different species of seabirds preferentially forage at different distances from the breeding colony on Ascension Island. Brown boobies (*Sula leucogaster*) forage closest to the island, masked boobies (*Sula dactylatra*) at intermediate distances, and Ascension frigatebirds (*Fregata aquila*) the furthest away. Weber et al. (2021) also provide evidence that these species all feed on flying fish, primarily tropical two-winged flying fish (*Exocoetus volitans*).

These observations by Weber et al. (2021) raise the questions of how decisions by individual birds and the coupled prey dynamics interact to generate patterns of prey depletion halos and distributions of foraging birds. Can this process actually lead to different species partitioning foraging space as a result of behavior and thereby allowing for robust coexistence on a single prey species? The described interactions are sufficiently entangled so that a mathematical analysis is required to obtain insights into these questions. Dukas and Edelstein-Keshet (1998) present a single species model for the ideal free distribution of central place foragers in a two-dimensional environment. They, however, do not include prey dynamics and their study therefore does not provide information about the shape of the prey-depletion halo induced by the ideal free distribution. Gaston et al. (2007) develop an energy budget model, showing how maximum colony size depends on seabird foraging traits, but again, they do not consider prey dynamics. Finally, Weber et al. (2021) consider a two-dimensional prey consumption and dispersion model, showing that their observed prey halo can in principle result from the seabirds breeding on Ascension Island, but they hold the multi-species predator distribution fixed. Thus, to date no model exists that describes the joint, endogenously generated distribution of central place foragers and their prey, or provides a mechanism leading to the coexistence of multiple species on the prey halo caused by their foraging activity.

We here address these questions by developing a mathematical model for multiple colonial bird species breeding on an isolated island (a variant of the model analyzing the distribution of foraging trips of colonial social insects is considered in Box 1). Prey dynamics in the two-dimensional surrounding of the island is modeled explicitly as a result of intrinsic birth and death, random movement in space and consumption by birds. We characterize the ideal free distribution of foragers maximizing the rate of prey delivery to their offspring in the presence of flight and search costs. The ideal free distribution determines the birds' foraging trips around the island and, in turn, prey dynamics and bird demography. The model is first analyzed by

considering a single species, identifying the joint equilibrium of the birds' colony size, the distribution of their foraging trips, and the resulting prey distribution. We show that prey depletion halos are a robust phenomenon and that the distribution of foraging trips is an unimodal function of distance from the island. We then consider the full model to investigate the conditions for coexistence of different bird species, where different species differ in their foraging traits under the assumption that these cannot be optimized simultaneously but are coupled by trade-offs. For instance, species that are good flyers, and thereby minimize energetic costs of long distances foraging trips, might be poorer at catching fish and vice versa. We show that robust coexistence of different bird species is easily obtained as a result of a multi-species idea free distribution where species behaviorally partition foraging space into mutually exclusive circular zones around the island.

2 Model

2.1 Biological assumptions

We consider a population of birds breeding on an isolated island. The number of successfully raised offspring depends on the amount of prey they catch by foraging in the surrounding ocean and that they are able to deliver back to their nestlings. The waters surrounding the island are assumed to be homogeneous and harbor a single prey species. Any two points at equal distance z from the island are assumed to be visited with equal probability by foraging birds. As a result, the distribution of prey is radially-symmetric around the island. We denote by $R(z)$ the equilibrium prey density at distance z and the total amount of prey at distance z then equals $2\pi z R(z)$.

A foraging trip starts with birds flying from the island to a point at distance z, where they start foraging. Individuals forage at a given distance until they catch a prey, that is, individuals are *single prey loaders* (we consider multiple prey loaders in Appendix A.1). After a successful catch, birds fly back to the island to deliver the prey to their nest. If birds fly with speed v, then it takes a flying time of $T_{\mathrm{f}}(z) = 2z/v$ time units to travel both directions.

The rate at which birds foraging at distance z catch prey is given by $aR(z)$, where a denotes the capture efficiency. The time it takes a bird to successfully catch a prey item at distance z is

then exponentially distributed with mean $T_s(R(z)) = 1/(aR(z))$, referred to as search time. If birds can extract on average b energy units from a single prey and if c_f and c_s denote the energy costs per time unit flying and searching, respectively, then

$$B(R(z), z) = b - c_f T_f(z) - c_s T_s(R(z)) \tag{1}$$

gives the net energy content of a prey item from distance z. In Appendix A.1 we show that with the above assumptions the rate at which birds deliver prey to the nest is given by

$$f(R(z), z) = \frac{aR(z)}{1 + aR(z)T_f(z)}, \tag{2}$$

which we recognize as Holling's type-II functional response (Holling, 1959). The net rate of energy uptake obtained from foraging at distance z, referred to as *payoff* and denoted $\Pi(z)$, equals the product of the prey delivery rate and the net energy content per prey and thus is

$$\Pi(z) = f(R(z), z)B(R(z), z). \tag{3}$$

Hence, payoff at distance z depends on prey density at that distance, both through the functional response and the net energy content.

We assume that there are no prey on the island (i.e., $R(0) = 0$). Away from the island, equilibrium prey density $R(z)$ at distance z depends on three processes. First, the prey growth rate $g(R(z))$ in the absence of predation, namely, birth minus predation-independent death. Second, prey move homogeneously in space at rate m (formally, we assume a *reaction-diffusion* process for the prey, see Appendix A.2 for details). Third, prey density is reduced due to mortality from foraging birds. Death through predation at distance z depends on how often an area at that distance is visited by birds, which, in turn, depends on the total number of birds and the probability that birds visit an area at distance z. In the absence of bird predation, prey have the same equilibrium density R^* everywhere around the island.

The probability of birds foraging at different distances is assumed to be an individual decision variable, which thus reflects the birds' choice. We denote by $p(z)$ the probability density that an individual forages at distance $z \in \mathbb{R}_+$ (i.e., $\int_0^\infty p(z)\,\mathrm{d}z = 1$) at a behavioral equilibrium. Our central behavioral assumption is that this equilibrium strategy is an ideal free distribution

determined by the payoff given by eq. (3). Thus, individuals are able to distribute themselves "freely" over the different foraging distances, such that their payoff from each distance where foraging occurs is the same and at least as high as at distances not visited (Fretwell and Lucas, 1970; Křivan et al., 2008). In a population consisting of N birds, the density of birds foraging at any point at distance z is equal to $p(z)N/(2\pi z)$ and the rate of prey depletion at that point is the product of this density and the functional response.

Finally, we assume that the average payoff

$$\bar{\Pi} = \int_0^\infty p(z)\Pi(z)\,\mathrm{d}z \tag{4}$$

to an individual at the ideal free distribution determines the number of successfully raised offspring. The average payoff thus affects the birds' population size and hence the number of competitors at any given distance. Without loss of generality, we assume that this energy is converted into offspring with an efficiency equal to one.

2.2 Equilibrium conditions for prey, bird behavior and demography

According to our assumptions, the equilibrium prey density $R(z)$, the ideal free distribution $p(z)$, and the equilibrium abundance N of birds are determined by the following coupled system of equations.

First, prey density at distance z reaches an equilibrium when its renewal is balanced by predation due to foraging birds at that distance. This is the case when

$$G(R(z),z) - f(R(z),z)\frac{p(z)N}{2\pi z} = 0, \tag{5}$$

where the second term on the left-hand side is the rate of prey removal at a point at distance z and

$$G(R(z),z) = g(R(z)) + m\left(\frac{\mathrm{d}^2R(z)}{\mathrm{d}z^2} + \frac{1}{z}\frac{\mathrm{d}R(z)}{\mathrm{d}z}\right) \tag{6}$$

is the prey renewal rate at that distance. The first term on the right-hand side of eq. (6) describes the prey's growth rate. In our numerical analysis, we consider two alternatives, logistic growth and constant prey renewal ("chemostat dynamics"). The second term describes movement (or

"diffusion"), which is proportional to the movement rate m and depends on the first and second derivative of the prey density with respect to distance z (see Appendix A.2 for why this is so).

Second, the behavior $p(z)$ is characterized as an ideal free distribution and thus by the fact that, given individuals in the population follow this behavior, the payoff to all individuals must be identical at all distances where they forage, and must be at least as high as the payoff individuals would obtain at distances where they do not forage. Thus,

$$\Pi(z) = \beta \qquad \text{for all } z \in \mathbb{R}_+ \text{ with } p(z) > 0 \tag{7a}$$

$$\Pi(z) \leq \beta \qquad \text{for all } z \in \mathbb{R}_+ \text{ with } p(z) = 0, \tag{7b}$$

where β is the constant payoff obtained from visited foraging distances (the interval of foraging distances satisfying eq. (7a) is the support of the ideal free distribution). Note that, while the payoff given by eq. (7) does not depend explicitly on $p(z)$ (recall eqs. 1-3), a dependence enters through eq. (5) as the payoff depends on the equilibrium prey density $R(z)$, which depends on the ideal free distribution expressed by all other individuals in the population. At the ideal free distribution characterized by eq. (7), the payoff obtained from foraging at any visited distance is no less than the payoff obtained from foraging at any possible distance (i.e., $\Pi(y) \leq \Pi(z)$ for all $y \in \mathbb{R}_+$ and all $z \in \mathbb{R}_+$ with $p(z) > 0$). This implies that when individuals in the population behave according to the ideal free distribution, no individual has an incentive to unilaterally change behavior and the ideal free distribution is equivalent to a Nash equilibrium (Cressman et al., 2004; Křivan et al., 2008). This makes the ideal free distribution a fundamentally relevant behavioral equilibrium concept.

Third, the number of foragers is at their demographic equilibrium N when birth balances death, that is, when the average payoff equals the death rate μ, which is here assumed to be constant,

$$\bar{\Pi} = \mu. \tag{8}$$

The birth rate as given by the average payoff depends on N indirectly through the dependence of the equilibrium prey density $R(z)$ on N (see eq. 5). Note that eq. (7) implies that the average payoff is $\bar{\Pi} = \beta$ and therefore, due to eq. (8), we have $\Pi(z) = \mu$ for all z with $p(z) > 0$.

The coupled system of equations (5)–(8) characterizes the prey equilibrium $R(z)$, the birds'

behavioral equilibrium $p(z)$ and their equilibrium abundance N. In the following section, we derive explicit expressions for this joint equilibrium.

3 Analysis

3.1 Single bird species: prey halo and ideal free bird distribution

We start by observing that the flying cost $T_\mathrm{f} = 2z/v$ monotonically increases with distance z. As a consequence, when holding $R(z)$ fixed, the functional response $f(R(z), z)$ (eq. 2), and therefore the payoff $\Pi(z)$ (eq. 3), decrease with z and go to zero as z becomes large. Hence, a maximal traveling distance z_max has to exist beyond which prey is left unconsumed, $p(z) = 0$ for $z > z_\mathrm{max}$. Beyond this maximum, the prey will therefore reach its equilibrium density in the absence of consumption, denoted R^*. The payoff at this maximum distance satisfies

$$f(R^*, z_\mathrm{max}) B(R^*, z_\mathrm{max}) = \mu. \tag{9}$$

Solving this equation for z_max, using eqs. (1)–(2), gives

$$z_\mathrm{max} = \frac{v\big(abR^* - \mu - c_\mathrm{s}\big)}{2aR^*(\mu + c_\mathrm{f})}. \tag{10}$$

Solving eq. (7) for $R(z)$, eq. (5) for $p(z)$ and using the equality $f(R(z), z) = \mu / B(R(z), z))$, the normalization $\int_0^{z_\mathrm{max}} p(z)\,\mathrm{d}z = 1$ along with $\Pi(z) = \mu$, we obtain

$$R(z) = \begin{cases} 0 & \text{for } z = 0 \\ \dfrac{\mu + c_\mathrm{s}}{a\left(b - \dfrac{2z}{v}(c_\mathrm{f} + \mu)\right)} & \text{for } 0 < z \leq z_\mathrm{max} \\ R^* & \text{for } z > z_\mathrm{max} \end{cases} \tag{11}$$

and

$$p(z) = \begin{cases} \dfrac{2\pi z}{N} \dfrac{B(R(z), z) G(R(z), z)}{\mu} & \text{for } 0 \leq z \leq z_\mathrm{max} \\ 0 & \text{for } z > z_\mathrm{max} \end{cases} \tag{12}$$

where

$$N = \frac{2\pi}{\mu} \int_0^{z_{\max}} zB(R(z), z)G(R(z), z)\,\mathrm{d}z. \tag{13}$$

Eqs. (12)–(13) provide an explicit representation of the joint equilibrium for prey, bird behavior and demography, since eq. (11) provides an explicit expression for $R(z)$, which, in turn, determines $p(z)$ and N. Figure 1(a) illustrates the shape of $R(z)$ and $p(z)$ as a function of distance from the island z.

The following conclusions can be drawn. First, eq. (11) shows that the equilibrium prey density $R(z)$ has its lowest value at $z = 0$, thereafter increases with increasing z, and eventually reaches the equilibrium in the absence of consumption, R^*. This is a prey depletion halo, a generic feature of our model. The shape of the halo depends only on the biology of the birds and thus neither on the details of prey renewal nor movement. This remarkable property has its counterpart in standard predator-prey theory, where the prey equilibrium density only depends on properties of the predator as long as the predator's functional response is independent of its own density (e.g., Iannelli and Pugliese, 2014, pp. 159). Second, the extent of the prey depletion halo, as given by $z_{\max}$, increases with the birds' flying speed v, the prey's energy content b, and the maximum prey density R^*, and decreases with flying and search costs, c_{s} and c_{f}, respectively. Third, in the absence of prey movement ($m = 0$) the ideal free distribution is a unimodal function of z that starts at zero and again reaches zero at $z = z_{\max}$ (blue curve in fig. 1a). Increasing the prey movement rate results in birds exploiting distances further away from the island more heavily, because diffusion results in a net movement of prey from distances with higher density to distances with lower prey density (see fig. B1 for the ideal free distribution for different search costs c_{s} and for constant prey renewal). Fourth, equilibrium colony size N, as given by eq. (6), increase with the prey's net energy content $B(R(z), z)$ and its renewal rate $G(R(z), z)$. Since $G(R(z), z)$ is linearly increasing in the movement rate m, so is the birds' equilibrium population size, as given in the legend of fig. 1(a).

3.2 Single bird species at fixed population size

In the above analysis, we assumed that the bird population is at its demographic equilibrium, emphasizing the fact that the area restricted foraging during breeding indeed sets the limit to colony size as hypothesized by Ashmole (1963). However, due to human disturbance, seabird

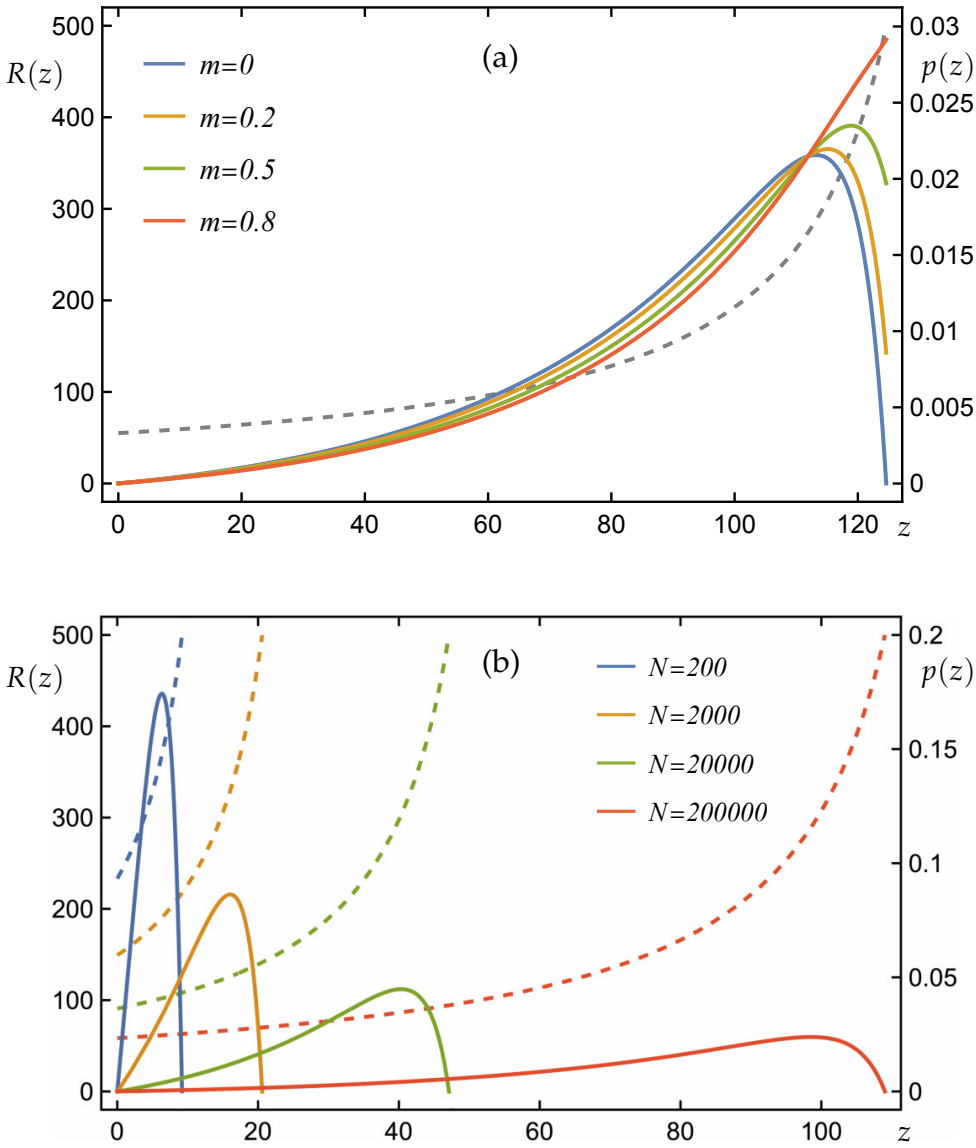

Figure 1: Equilibrium prey density $R(z)$ (hatched lines, left y-axis) and ideal free distribution $p(z)$ (solid colored lines, right y-axes) as a function of distance z from the island under logistic prey growth ($g(R(z)) = R(z)(r - \alpha R(z))$, where r is the intrinsic per-capita growth rate and α the sensitivity to competition). (a) Results under the assumption that birds have reached their demographic equilibrium for four different values of the movement rate m. The ideal free distribution $p(z)$ is an unimodal function in z for small m and becomes monotonically increasing for larger m. For the parameters given below, in the order of increasing values of the movement rate m, the equilibrium colony size N equals 288 858, 307 085, 334 427 and 361 768. (b) Results for four different fixed population sizes N. Prey depletion halo's become more pronounced and birds fly larger distances with increasing population size. Parameter values: $r = 0.02$, $\alpha = 0.00004$, $b = 1$, $c_f = 0.2$, $c_s = 0.5$, $a = 0.01$, $v = 70$, (A) $\mu = 0.05$, (B) $m = 0$.

populations are not necessarily at this equilibrium (e.g., Hughes et al., 2008). In this section, we extend our analysis to the case that the bird population size is fixed for a number N that is not equal to the demographic equilibrium. This allows us to make predictions about the extent of prey depletion halos depending on current population size. In this case, the mean payoff β has to fulfill the constraint $\bar{\Pi} = \beta$, where β is an unknown quantity. Replacing μ with β in the expression for the maximum flying distance $z_{\max}$ given by eq. (10), the integral on the right-hand side of eq. (4) can be solved. This results in an implicit equation for β that can then be solved numerically given a population size. Once the value of β is obtained, eqs. (11) (again, after replacing μ with β) and (12) provide an explicit solution for the ideal free distribution $p(z)$ and the equilibrium prey density $R(z)$. The result is shown in fig. 1(b) for four different population sizes N. This figure shows that the maximum flying distance roughly doubles with each ten-fold increase in population size (for the population sizes 200, 2000, 20000, and 200000 the corresponding values of $z_{\max}$ are 9.2, 20.6, 47.1, and 109.0). This result is in qualitative agreement with the empirically determined distributions shown in fig. 2(b) of Patterson et al. (2022) for two species of murres (*Uria* spp.) when taking from their study the distances up to where 95% of the foraging trips occur.

The payoff β at the ideal free distribution for the above population sizes are 1.83, 0.99, 0.41, and 0.08, respectively. This exemplifies Ashmole's idea (Ashmole, 1963) that the rate of prey delivery to nestling decreases with increasing population size (as supported by several empirical studies (Hunt et al., 1986; Lewis et al., 2001; Ainley et al., 2004; Ballance et al., 2009).

We note that for fixed N the equilibrium prey density distribution $R(z)$ is no longer independent of the movement rate m. This is illustrated in fig. C1. Higher values of m result in a shorter maximal flying distance and a higher prey abundance at each distance z. This is in qualitative agreement with simulation results by Weber et al. (2021, their fig. 3B).

3.3 Multiple bird species and behavioral niche partitioning

In the above analysis, we considered a single bird species. However, in many seabird colonies, different species coexist. Weber et al. (2021) observed that on Ascension Island three investigated bird species focus for their foraging trips on different distances from the breeding colony. This observation is maybe not surprising, given that species differ in morphological and physiological

traits that affect the costs and benefits of foraging trips to areas at different distances from the colony. For instance, Gaston et al. (2007) show how traits such as flying speed and energy costs for flying and feeding affect maximum flying distance and the minimum energy requirement that needs to be obtained from foraging at different distances. Here, we formalize this idea by assuming that birds are characterized by a quantitative trait x ($x \in \mathbb{R}$) that can affect their feeding efficiency a, their flying speed v, and their flying and search costs, c_{f} and c_{s}, respectively, to which we refer collectively as foraging components. Individuals of the same species have the same trait value x so that species differ in their foraging components (but we assume that they have the same death rate μ). A natural assumption is then that the performance in different tasks is subject to trade-offs. For instance, a morphology allowing for a high flying speed v might be less efficient at foraging by plunge-diving and therefore would be coupled to a lower feeding efficiency a. In the following, we show that such trade-offs indeed allow for the coexistence of multiple seabird species through a partitioning of the waters surrounding the colony into distinct circular foraging zones.

In order to indicate that the foraging components can differ with x, we henceforth write these as functions of x, for instance, $a(x)$. Similarly, we add the argument x to the payoff function (eq. 3, $\Pi(x,z)$), the maximum flying distance (eq. 10, $z_{\max}(x)$), the equilibrium prey abundance (eq. 11, $R(x,z)$), the ideal free distribution (eq. 12, $p(x,z)$), and the equilibrium bird population size (eq. 13, $N(x)$) to indicate that these functions depend on the birds' phenotype.

Two see how trait differences allow for coexistence, we start by observing that a species with trait value x induces a corresponding equilibrium prey density curve $R(x,z)$ (in the absence of any other species). Figure 2(a) shows such curves for four trait values x under the assumption that feeding efficiency and flying speed are negatively correlated ($a(x)$ is a monotonically increasing function while $v(x)$ is a monotonically decreasing function in x). This figure shows that for any two species, the curves $R(x,z)$ intersect exactly once. For illustration, let us focus on two species, say, those characterized by $x_1 = 3$ (henceforth called species 1, blue curve) and $x_2 = 1$ (henceforth called species 2, orange curve). We see that $R(x_1,z) < R(x_2,z)$ in the interval $[0,z_1]$, where $z_1 \approx 40$ is the point of intersection of the two equilibrium prey density curves, and $R(x_2,z) < R(x_1,z)$ in the interval $[z_1, z_{\max}(x_2)]$. The fact that $R(x_1,z) < R(x_2,z)$ in the interval $[0,z_1]$ implies that the payoff, and thus the birth rate, to species 2 is lower than the death rate.

As a consequence, species 2 does not forage in this interval (as described by eq. 7b). Indeed, if $R(x_1, z) < R(x_2, z)$ at z, then $\Pi(x_2, z) < \mu$ and therefore $p(x_2, z) = 0$ must hold. As a result, the interval $[0, z_1]$ is only utilized by species 1 while the interval $[z_1, z_{\max}(x_2)]$ is only utilized by species 2. We obtain a partitioning of the surrounding of the colony where species 1 only exploits distances close to the island and species 2 only exploits distances further away from the island. Hence, the species with the trait value inducing the lowest equilibrium prey density in a foraging interval exclude species with other trait values. This argument, which is developed more formally in Appendix C.3, echoes the resource-ratio rule of community ecology. It states that if multiple species compete for a single limiting resource, here the resource at distance z, then whichever species can survive at the lowest equilibrium resource level outcompetes all others (Tilman, 1982; Grovers, 1997), resulting in competitive exclusion (Levin, 1970).

For two species to indeed be able to coexist, it is a necessary (and sufficient) requirement that the corresponding equilibrium prey density curves $R(x, z)$ intersect with each other. In Appendix C.2, we show that two curves $R(x, z)$ intersect at most once. Therefore, two curves $R(x, z)$ intersect with each other if and only if the values of the equilibrium prey density at distance $z = 0$ ($R(x, 0)$) and the maximum flying distance $z_{\max}(x)$ have the same ordering. For our example above, fig. 2 shows that $R(x_1, 0) < R(x_2, 0)$ and $z_{\max}(x_1) < z_{\max}(x_2)$. Thus, the trade-off between foraging components induces a trade-off in the efficiency to forage at short and long distances from the colony. Species 1, having a higher capture efficiency, is more efficient at exploiting prey close to the colony, resulting in a lower equilibrium prey density at $z = 0$, at the cost of having a shorter maximum traveling distance, while for species 2, having a higher flying speed, the situation is reversed.

In Appendix C.3, we show that the above arguments generalize to any finite community $\mathcal{X} = \{x_1, x_2, ..., x_n\}$ with $n > 2$ (fig. 2 shows it for $n = 4$). Thus, whenever we have coexistence of a set of species, they forage in mutually exclusive distance intervals around the island (until a distance is reached beyond which no individual forages), each species occupying exactly one interval. In each interval, the prey distribution is determined by the foraging components, and thus the trait value x, of the species occupying that interval according to eq. (11). The corresponding ideal free distribution and abundance of that species are given by analogues of eqs. (12)–(13), where the ideal free distributions of each species ranges over intervals that depend on the trait

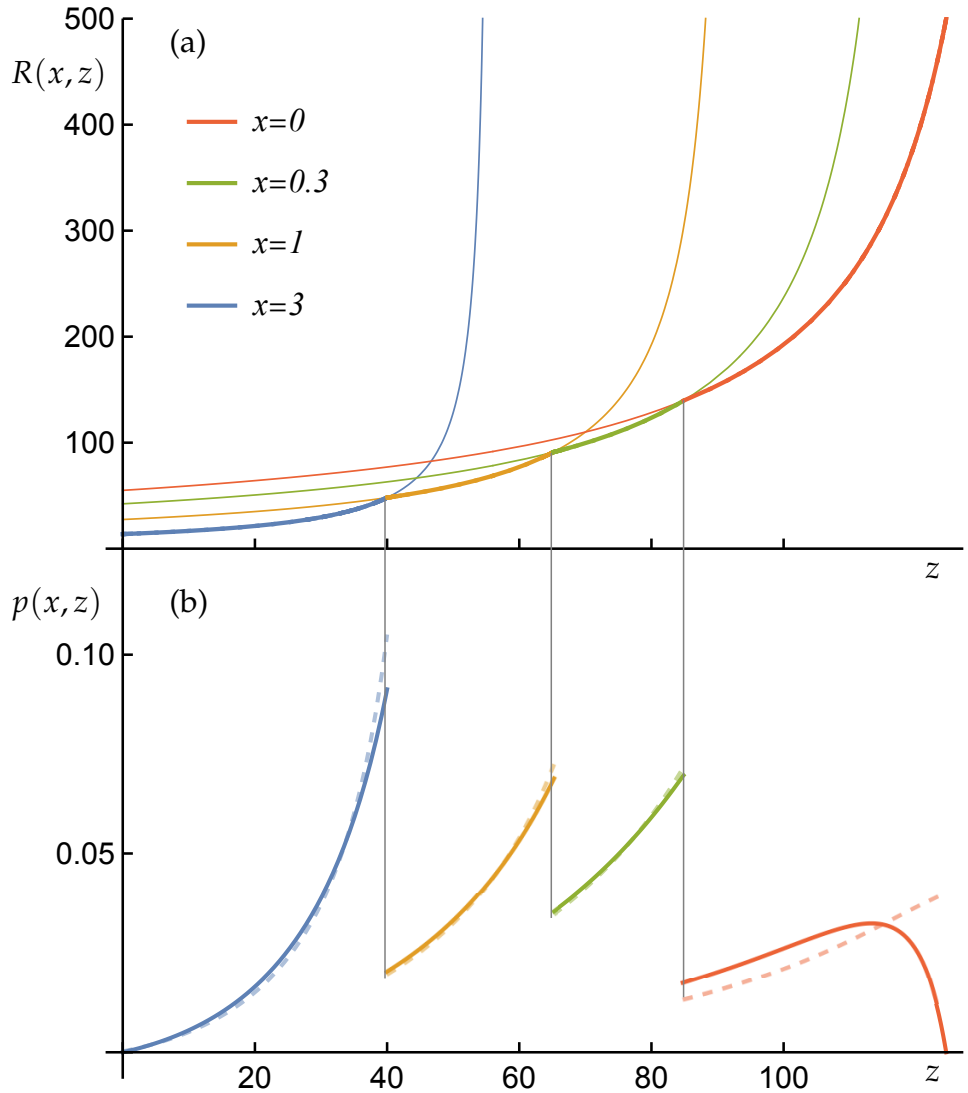

Figure 2: Equilibrium prey density $R(x,z)$ in (a) and ideal free distribution $p(x,z)$ in (b) as a function of distance z from the island for four different trait values x. The equilibrium prey density curve with the lowest value is shown as a thick line. Due to competitive exclusion, bird species differing in their trait value x only forage at distances where they reduce prey density to a lower level than the other species, resulting in the multi-species ideal free distribution shown in (b) and a multi-species prey depletion halo, given by the composite thick line in (a). Grey vertical lines, connecting panel (a) and (b), are drawn at the z-values where species identity changes. The ideal free distribution is shown for two values of the movement rate; solid lines correspond to $m = 0$ and hatched lines to $m = 0.8$. Parameter values as in fig. 1(a), except that the values for a and v are now trait dependent according to the functions $a(x) = a_0 + a_1 x$ and $v(x) = v_0/(1 + v_1 x)$, respectively, with $a_0 = 0.01$, $a_1 = 0.01$, $v_0 = 70$, $v_1 = 0.5$.

values of all other species in the community (see eqs. C12–C14). The result is a multi-species prey depletion halo, as shown in fig. 2(a), and a multi-species ideal free distribution, as shown in fig. 2(b). Hence, our main finding is that, in the presence of trade-offs between foraging components, multiple bird species can coexist on a single prey species through behavioral niche partitioning into discrete distance intervals. Just as in the single-species case, prey movement does not affect the equilibrium prey distribution. As a consequence, prey movement does not affect the partitioning of distances of coexisting bird species. However, just as in the single species case, prey movement results in a shift of the ideal free distribution of each species towards higher distances due to a net movement of prey individuals toward distances with lower prey density (see fig. 2b).

Figure 2 is based on the assumption that capture efficiency $a(x)$ and flying speed $v(x)$ are negatively correlated. In Appendix D, we determine for all possible pairwise trade-offs between foraging components whether they have the potential to induce a trade-off between $R(0, x)$ and $z_{\max}(x)$, which is the prerequisite for species coexistence (allowing for more than two foraging components to vary with x does not result in qualitative new results). The result is summarized in table 1. Two different outcomes occur. First, a trade-off between foraging components does not induce a trade-off in the efficiency to forage at different distances. This case is illustrated in fig. D1. Second, whether a trade-off between foraging components induces a trade-off between $R(0, x)$ and $z_{\max}(x)$ depends on parameter and trait values. Figure 2 shows an example where indeed four species can coexist, while fig. C2 shows an example where coexistence is possible for some species but not for others.

Table 1: The four foraging components feeding efficiency a, flying speed v, flying costs c_{f} and search costs c_{s} allow for six different pairwise combinations. For each combination, we determine whether a negative correlation between the foraging components has the potential to mediate coexistence of species with different trait values x. See Appendix D for details.

coexistence	a & v	a & c_{f}	a & c_{s}	v & c_{f}	v & c_{s}	c_{f} & c_{s}
parameter-dependent	✓	✓			✓	✓
not possible			✓	✓		

The results from Table 1 can be understood as follows. Foraging comes with two costs (see eq. 1), namely costs associated with flying ($c_{\mathrm{f}} 2z/v$) and costs associated with searching for prey ($c_{\mathrm{s}}/(aR(z))$). Flying costs increase and search costs decrease with distance z from the island. The

latter is a consequence of the prey depletion halo around the island. Different species can coexist if they are specialized to forage on different distances from the island by either experiencing low costs when foraging on depleted prey close to the island (high a or low c_s) at the cost of higher costs when foraging on less depleted prey further away from the island (low v or high c_f) or vice versa (high v or low c_f at the cost of low a or high c_s).

4 Discussion

Inspired by the evidence provided by Weber et al. (2021) for (i) a prey depletion halo around the seabird colony on Ascension Island and (ii) the spatial partitioning of the feeding grounds surrounding the colony between coexisting seabirds, we here present a comprehensive mathematical model studying the distribution of foraging trips of central place foragers exploiting a single prey species in a two-dimensional environment around an island. By solving the joint equilibrium of the prey distribution, the behavioral dynamics of the forager and its demography, we show that a prey depletion halo is a robust outcome of central place foraging. Its shape, given by eq. (11) and illustrated in Figs. 1 and 2, is robust in the sense that it is independent of the specifics of the prey's population dynamics, including its movement rate, as all parameters in eq. (11) describe properties of the forager.

Our full model includes an arbitrary number of species, where, due to species-specific morphological and physiological trait values, individuals can differ in flying speed, feeding efficiency, travel and search costs. We show that coexistence is a robust outcome that obtains whenever species differences result in some species experiencing lower costs when foraging on a prey at low density close to the breeding colony, while others experience lower costs when flying long distances to forage on a prey at high density. A qualitatively similar result has been found by Bolin et al. (2018) in a model describing the foraging behavior of solitary bees, assuming that species vary along a trade-off of low flight costs and efficient resource use. We want to stress that, in contrast to Bolin et al. (2018), coexistence in our model occurs in the presence of a single biological prey species. As explained above, the key to understand this coexistence is that for different species the same prey — but at different distances from the colony — comes with different costs. The result is a multi-species ideal free distribution (fig. 2b) and a multi-species prey depletion halo (fig. 2a), where no two bird species forage at the same distance. Instead,

different species exploit mutually exclusive circular zones around the island (see Appendix C.3 for a proof). This sorting of species into mutually exclusive foraging zones occurs despite the fact that, in principle, the area in the vicinity of the colony would be preferred by all species since it is here that catching prey comes at the lowest travel costs, both in terms of the time needed to reach the foraging area and the energy investment to do so. It is in the presence of competitors that deplete prey to such low values such that the immediate surrounding of the colony is not sufficiently profitable to be used by species that are less efficient foragers. Thus, for each species, the fundamental niche consists of the circular area around the colony that is limited by the species specific maximum flying distance. However, in the presence of competitors, the realized niche of each species consists of the circular zone around the island where that species is able to deplete the prey to a lower density than any other species. A community of coexisting species in our model is an example of a community with *shared preferences* (Rosenzweig 1991, fig. 7; Mittelbach and McGill 2019, Box 8.1; see Wisheu 1998 for a review). This thus differs from classical theory based on *distinct preferences* where each species is optimal in a different part of niche space, as developed by Robert MacArthur and colleagues (MacArthur and Levins 1967; MacArthur 1972; see Case 2000; Mittelbach and McGill 2019; Begon and Townsend 2021 for textbook treatments).

A consequence of the fact that coexistence results from behavioral niche partitioning is that the conditions for coexistence are relatively mild compared to models where coexistence is only mediated by trait differences without linked behavioral differences. A corresponding result has been found in a model where consumers compete for two resources and where individuals can choose to either attack or ignore a prey item, depending on their expected energy gain from doing so, which depends both on their phenotype and on the abundance of resources as determined by the competitors (Rueffler et al., 2007). In that model, optimal diet choice greatly enlarges the set of pairs of trait values that allow for coexistence. Furthermore, coexistence in our model is generally not a transient phenomenon if one allows for evolutionary change in the trait values x that characterize the different species. This can be seen from fig. 2. Changes in the trait value x of the four coexisting species changes the pattern of intersections of the equilibrium prey density curves only quantitatively but not qualitatively. Thus, coexistence does not easily break down under evolutionary change. In fact, the opposite is likely to be true, an input of individuals with different trait values, either by mutation or immigration, can readily increase diversity, since an

incoming species with a different trait value is unlikely to decrease the equilibrium prey density at all distances (see eq. (D9) for the condition under which this is true for the case that flying speed and feeding efficiency are trait-dependent, the case illustrated in Figs. 1–2 and C2).

Weber et al. (2021) report the distribution of seabirds both as the proportion of time birds spend foraging at different distances from the island (their fig. 2A) and as relative density (their fig. 2B). The first corresponds to the ideal free distribution, as shown in fig. 2(b). Obviously, their distribution markedly differs from ours. This is not surprising since our derivation assumes that foragers are "ideal", that is, that they have complete information about both their environment and their own abilities. This is certainly not true for natural systems, where individuals have to build up this information through constant probing. Furthermore, intraspecific phenotypic variance occurring in natural populations could cause that different individuals of the same species slightly differ in their foraging decisions, while in our model all individuals of the same species are identical. In Appendix B, we discuss how our results approximate the empirical foraging distributions reported in Weber et al. (2021) when expressed as relative densities.

It is noteworthy that our model is agnostic as to whether the ideal free distribution is composed of individuals that all distribute their foraging trips according to the ideal free distribution (mixed strategy) or of individuals that each utilize a single distance and that the frequency distribution of individuals utilizing the different distances follows the ideal free distribution (mixture of pure strategies). This pure-mixed strategy equivalence occurs since what determines energy intake at a given distance is the realized density of individuals at that distance, and that at the ideal free distribution the net energy gain is the same at all visited distances. It would be interesting to analyze the behavior of individuals that are radio-tracked from this perspective. It is, for example, conceivable that individuals adapt to different distances through some type of learning, leading to a behavior more akin to a pure strategy at the individual level.

Finally, we want to emphasize that our results are obtained under the assumption that birds act as individual payoff maximizers. Central place foragers that are selected to maximize group payoff, such as colonies of social insects consisting of highly related individuals, do not follow an ideal free distribution (see fig. 4). Instead, we show that colony payoff is maximized by increasing maximum travel distance and simultaneously underexploiting the vicinity of the colony.

4.1 Conclusion

In his influential study of seabirds on Ascension Island, Ashmole (1963) proposed that seabirds breeding in large colonies locally reduce their prey, generating a prey depletion halo around the colony. Strong evidence for such halos has been provided by Weber et al. (2021), a study that further suggests that coexistence of seabirds is made possible by individual foraging decisions resulting in a spatial segregation into different circular zones around the colony. Our model shows that prey depletion halos are a robust outcome, suggesting they should generally be associated with central place foraging and extend beyond seabird ecology. We also show that trait mediated behavioral niche partitioning results in robust coexistence. We suggest that this process facilitates species coexistence compared to standard theory based on trait-mediated niche partitioning as developed in the wake of MacArthur and Levins (1967)'s seminal work. Trait-dependent ideal free distributions are not limited to central place foragers and may play a more general role as a coexistence promoting mechanism.

Box 1: Group versus individual foragers

The results in the main section are derived under the assumption that selection acts to maximize individual payoff. For highly related social insects, however, it is appropriate to assume that there is no conflict between group members and selection acts to maximize colony payoff. Here, we consider a central-place foraging model for such foraging groups, where we search for the behavioral strategy $p(z)$ that maximizes the net per-capita rate of energy uptake of group members. Our results are based on a non-self-renewing resources, such as nectar in flowers. The equilibrium behavior $p(z)$ maximizing group payoff is derived in Appendix E, using all biological assumptions of the individual foraging model, except that (i) group size is N fixed, and (ii) movement of resources is absent ($m = 0$).

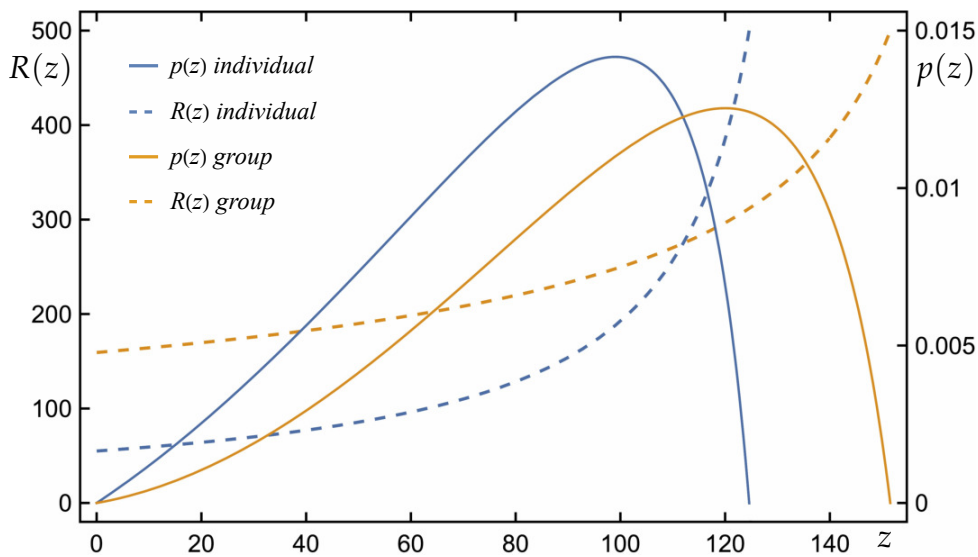

Figure 3: Equilibrium prey density $R(z)$ (hatched lines, left y-axis) and foraging distribution $p(z)$ (solid lines, right y-axes) for individual (in blue) and group foragers (in orange) under constant resource renewal ("chemostat dynamics"; $g(R(z)) = b_R - d_R R(z)$, where b_R and d_R, are the constant resource renewal and per capita death rate, respectively). For the used parameters, equilibrium population size of individual foragers equals $N = 36859$, and this value is used as a parameter for group foragers. Hence, given equal population size, group foragers use distances close to the colony less intensively and instead utilize a larger area around the colony ($z_{max} = 152$ for group foragers vs. $z_{max} = 125$ for individual foragers). Note that the two curves for $R(z)$ and for $p(z)$ intersect with each other at the same value ($z = 112$). The reason is that the resource equilibrium density at distance z is a direct consequence of the number of individuals foraging at that distance. Parameters in the resource renewal function $g(R(z))$: $b_R = 0.4$ and $d_R = 0.0008$. All other parameters as in fig. 1.

We find that at the group foraging equilibrium, the maximum travel distance is larger and the distribution of travel distances is more skewed toward large distances compared to the equilibrium for individual foragers (fig. 3). Thus, group foragers exploit regions close

to the colony less intensely and instead use a larger foraging area. As a result, group foragers do not equalize payoffs at different distances but distribute themselves such that payoffs at short distances exceeds payoffs at long distances (fig. 4), generalizing results from two-patch models by Brown (1998), Dukas and Edelstein-Keshet (1998), and Morris et al. (2001), and from a simulation study by Robinson et al. (2022). This can be explained by the avoidance of kin competition at distances close to the colony where travel costs are lowest. By exploiting resources at large distances, group foragers decrease competition for relatives foraging close to the colony. The increase in payoff due to this decrease in competition more than outweighs the decrease in payoff suffered by individuals from increased competition far away from the colony and by individuals flying further than the maximum travel distance of individual foragers, resulting in higher average payoff under group foraging ($\bar{\Pi} = 0.096$ compared to $\bar{\Pi} = 0.05$ under individual foraging). Thus, group foragers exploit resources more efficiently. Both these trends, decreases in payoff with distance and higher average payoff, are expected to be robust outcomes under group foraging, since they are both direct consequences of the reduced competition entailed by maximizing group payoff.

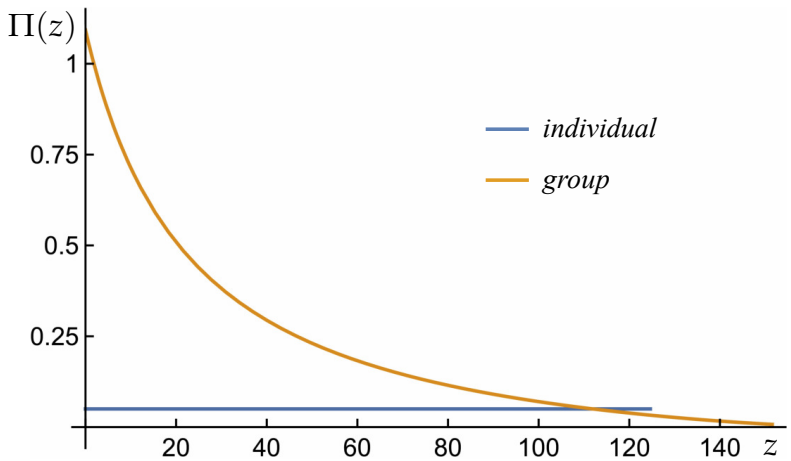

Figure 4: Payoff $\Pi(z)$ for group (in orange) and individual (in blue) foragers. As a result of the ideal free distribution, individual foragers have an identical payoff at all distances (equal to $\mu = 0.05$, up to $z_{\max} = 125$). In contrast, group foragers under-exploit resources at short distances and over-exploit resources at large distances (fig. 3). As a result, individual payoff is monotonically decreasing with distance z (up to $z_{\max} = 152$). The two payoff curves $\Pi(z)$ intersect with each other at the same distance as the equilibrium resource curves ($z = 112$, cf. Fig.3), as payoff is a direct consequence of resource abundance. Parameters as in fig. 3.

References

Ainley, D. G., C. A. Ribic, G. Ballard, S. Heath, I. Gaffney, B. J. Karl, K. J. Barton, P. R. Wilson, and S. Webb. 2004. Geographic structure of adélie penguin populations: Overlap in colony-specific foraging areas. Ecological Monographs 74:159–178.

Ashmole, N. P. 1963. The regulation of numbers of tropical oceanic birds. Ibis 103B:458–473.

Ballance, L. T., D. G. Ainley, G. Ballard, and K. Barton. 2009. An energetic correlate between colony size and foraging effort in seabirds, an example of the adélie penguin *Pygoscelis adeliae*. Journal of Avian Biology 40:279–288.

Begon, M., and C. R. Townsend. 2021. Ecology: From Individuals to Ecosystems. 5th ed. Wiley.

Birt, V. L., T. P. Birt, D. Goulet, D. K. Cairns, and W. A. Montevecchi. 1987. Ashmole's halo: direct evidence for prey depletion by a seabird. Marine Ecology - Progress Series 40:205–208.

Bolin, A., H. G. Smith, E. V. Lonsdorf, and O. Olsson. 2018. Scale-dependent foraging tradeoff allows competitive coexistence. Oikos 127:1575–1585.

Brown, J. S. 1998. Game Theory and Animal Behavior, chap. Game Theory and Habitat Selection, pages 188–220. Oxford University Press.

Bryson, A. E., and Y.-C. Ho. 1975. Applied Optimal Control: Optimization, Estimation and Control. CRC Press, New York.

Cairns, D. K. 1992. Population regulation of seabird colonies. Chap. 2, pages 37–61 *in* D. M. Power, ed. Current Ornithology, vol. 9. Springer New York.

Case, T. J. 2000. An Illustrated Guide to Theoretical Ecology. Oxford University Press.

Coulson, J. C. 2002. Colonial breeding in seabirds. *In* E. A. Schreiber and J. Burger, eds., Biology of Marine Birds. CRC Press.

Cressman, R., V. Křivan, and J. Garay. 2004. Ideal free distributios, evolutionary games, and population dynamics in multiple-species environments. The American Naturalist 164:473–489.

Dukas, R., and L. Edelstein-Keshet. 1998. The spatial distribution of colonial food provisioners. Journal of Theoretical Biology 190:121–134.

Edelstein-Keshet, L. 1988. Mathematical Models in Biology. The Random House/Birkhäuser Mathematics Series.

Elliott, K. H., K. J. Woo, A. J. Gaston, S. Benvenuti, L. Dall'Antonia, and G. K. Davoren. 2009. Central-place foraging in an arctic seabird provides evidence for storer-ashmole's halo. The Auk 126:613–625.

Forero, M. G., J. L. Tella, K. A. Hobson, M. Bertellotti, and G. Blanco. 2002. Conspecific food competition explains variability in colony size: A test in magellanic penguins. Ecology 83:3466–3475.

Fretwell, S. D., and H. J. Lucas. 1970. On territorial behavior and other factors influencing habitat distribution in birds. Acta Biotheoretica 19:16–36.

Furness, R. W., and T. R. Birkhead. 1984. Seabird colony distributions suggest competition for food supplies during the breeding season. Nature 311:655–656.

Furness, R. W., and P. Monaghan. 1987. Seabird Ecology. Chapman and Hall, New York.

Gaston, A. J., R. C. Ydenberg, and G. E. J. Smith. 2007. Ashmole's halo and population regulation in seabirds. Marine Ornithology 35:119–126.

Grovers, J. P. 1997. Resource Competition. Chapman and Hall, New York.

Holling, C. S. 1959. Some characteristics of simple types of predation and parasitism. The Canadian Entomologist 91:385–398.

Hughes, B. J., G. R. Martin, and S. J. Reynolds. 2008. Cats and seabirds: effects of feral domestic cat *Felis silvestris catus* eradication on the population of sooty terns *Onychoprion fuscata* on Ascension Island, South Atlantic. Ibis 150:122–131.

Hunt, J., George L., Z. A. Eppley, and D. C. Schneider. 1986. Reproductive Performance of Seabirds: The Importance of Population and Colony Size. The Auk 103:306–317.

Iannelli, M., and A. Pugliese. 2014. An Introduction to Mathematical Population Dynamics. Springer.

Křivan, V., R. Cressman, and C. Schneider. 2008. The ideal free distribution: A review and synthesis of the game-theoretic perspective. Theoretical Population Biology 73:403–425.

Levin, S. A. 1970. Community equilibria and stability, and an extension of the competitive exclusion principle. American Naturalist 104:413–423.

Lewis, S., T. N. Sherrat, K. C. Hamer, and S. Wanless. 2001. Evidence of intra-specific competition for food in a pelagic seabird. Nature 412:816–819.

MacArthur, R. H. 1972. Geographical Ecology. Harper & Row, NY.

MacArthur, R. H., and R. Levins. 1967. The limiting similarity, convergence, and divergence of coexisting species. The American Naturalist 101:377–385.

Mitchell, P. I., S. F. Newton, N. Ratcliffe, and T. E. Dunn, eds. 2004. Seabird Populations of Britain and Ireland: results of the Seabird 2000 census (1998-2002). T and A.D. Poyser, London.

Mittelbach, G. G., and B. J. McGill. 2019. Community Ecology. 2nd ed. Oxford University Press.

Morris, D. W., P. Lundberg, and J. Ripa. 2001. Hamilton's rule confronts ideal free habitat selection. Proceedings of the Royal Society London B 268:921–924.

Patterson, A., H. G. Gilchrist, S. Benjaminsen, M. Bolton, A. S. Bonnet-Lebrun, G. K. Davoren, S. Descamps, K. E. Erikstad, M. Frederiksen, A. J. Gaston, J. Gulka, J. Hentati-Sundberg, N. P. Huffeldt, K. L. Johansen,

A. L. Labansen, J. F. Linnebjerg, O. P. Love, M. L. Mallory, F. R. Merkel, W. A. Montevecchi, A. Mosbech, O. Olsson, E. Owen, N. Ratcliffe, P. M. Regular, T. K. Reiertsen, Y. Ropert-Coudert, H. Strøm, T. L. Thórarinsson, and K. H. Elliott. 2022. Foraging range scales with colony size in high-latitude seabirds. Current Biology 32:3800–3807.e3.

Robinson, S. V. J., S. E. Hoover, S. F. Pernal, and R. V. Cartar. 2022. Optimal distributions of central-place foragers: honey bee foraging in a mass flowering crop. Behavioral Ecology 33:386–397.

Rosenzweig, M. L. 1991. Habitat selection and population interactions: The search for mechanism. The American Naturalist 137:S5–S28.

Rueffler, C., T. J. M. Van Dooren, and J. A. J. Metz. 2007. The interplay between behavior and morphology in the evolutionary dynamics of resource specialization. The American Naturalist 169:E34–E52.

Seierstad, A., and K. Sydsæter. 1987. Optimal control Theory With Economic Applications. North-Holland, Amsterdam.

Sydsæter, K., P. Hammond, A. Seierstad, and A. Strøm. 2008. Further Mathematics for Economic Analysis. 2nd ed. Prentice Hall, Essex.

Sydsæter, K., and P. J. Hammond. 1995. Mathematics for Economic Analysis. Prentice-Hall.

Tilman, D. 1982. Resource Competition and Community Structure. Princeton University Press, New Jersey.

Weber, S. B., A. J. Richardson, J. Brown, M. Bolton, B. L. Clark, B. J. Godley, E. Leat, S. Oppel, L. Shearer, K. E. R. Soetaert, N. Weber, and A. C. Broderick. 2021. Direct evidence of a prey depletion "halo" surrounding a pelagic predator colony. Proceedings of the National Academy of Sciences 118:e2101325118.

Wisheu, I. C. 1998. How organisms parition habitats: different types of communty organization can produce identical patterns. Oikos 83:246–258.

Appendix A Model components

Throughout this appendix, our notation makes explicit that each bird is characterized by a quantitative trait $x \in \mathbb{R}$ and is part of a community consisting of n different species whose trait values are collected in the set $\mathcal{X} = \{x_1, x_2, \ldots, x_n\}$.

Appendix A.1 Rate of energy uptake by birds

We here derive the payoff function given by eq. (2) in the main part. Payoff is defined as the net rate of energy uptake of an individual foraging at distance z. A foraging trip consists of two activities, flying from the island to a foraging area at distance z and back, and searching for prey at that distance. We here assume that birds fly back to the island after catching n_{L} prey items, that is, they are n_{L}-prey loaders. All results in the main text are for single-prey loaders ($n_{\mathrm{L}} = 1$). We here show that this does not restrict the generality of the model. Let $T_{\mathrm{f}}(x, z)$ be the time it takes an individual with trait value x to fly from the island to distance z and back and $T_{\mathrm{s}}(x, z)$ the average time for that individual to successfully catch n_{L} prey items when foraging at distance z. Thus, the total time per foraging trip is $T_{\mathrm{f}}(x, z) + T_{\mathrm{s}}(x, z)$. Furthermore, let $E(x, z)$ be the net amount of energy gained during such a foraging trip. The net energy gain per time unit is then

$$\Pi(x, z) = \frac{E(x, z)}{T_{\mathrm{f}}(x, z) + T_{\mathrm{s}}(x, z)}. \tag{A1}$$

We assume that birds catch prey at rate $a(x)R(z)$, where $a(x)$ is the capture efficiency of an individual with trait value x and $R(z)$ the equilibrium prey density at distance z. Furthermore, each prey item contains on average b energy units. The net amount of energy gained during a foraging trip is then given by

$$E(x, z) = ba(x)R(z)T_{\mathrm{s}}(x, z) - c_{\mathrm{f}}(x)T_{\mathrm{f}}(x, z) - c_{\mathrm{s}}(x)T_{\mathrm{s}}(x, z), \tag{A2}$$

where $c_{\mathrm{f}}(x)$ and $c_{\mathrm{s}}(x)$ are the energy costs per time unit spend flying and foraging, respectively. The mean waiting time until n_{L} prey items are caught is $T_{\mathrm{s}}(x, z) = n_{\mathrm{L}}/(a(x)R(z))$. This follows from the rule for compounding exponential distributions, since the mean waiting time for a single catch is exponentially distributed with mean $1/(a(x)R(z))$. Substituting the expression

for $E(x,z)$ and $T_\mathrm{s}(x,z)$, eq. (A1) we obtain

$$\Pi(x,z) = \frac{a(x)R(z)\big(b - c_\mathrm{f}(x)T_\mathrm{f}(x,z)/n_\mathrm{L}\big) - c_\mathrm{s}(x)}{1 + a(x)R(z)T_\mathrm{f}(x,z)/n_\mathrm{L}}. \tag{A3}$$

This can be rewritten as

$$\Pi(x,z) = f(x,R(z),z)B(R(z),z), \tag{A4}$$

where

$$f(x,R(z),z) = \frac{a(x)R(z)}{1 + a(x)R(z)T_\mathrm{f}(x,z)/n_\mathrm{L}} \tag{A5}$$

is the functional response of an individual foraging at distance z, and

$$B(R(z),z) = b - c_\mathrm{f}(x)\frac{T_\mathrm{f}(x,z)}{n_\mathrm{L}} - c_\mathrm{s}(x)\frac{T_\mathrm{s}(x,z)}{n_\mathrm{L}} \tag{A6}$$

is the net energy content of a prey item at that distance. For $n_\mathrm{L} = 1$ and dropping the explicit dependence on the trait x in all functions, this yields eq. (2) in the main text. Note that $n_\mathrm{L} > 1$ does not qualitatively affect the functional form of the model, since n_L only scales the foraging times and scales them equally.

Appendix A.2 Reaction-diffusion process for the prey

We here derive eq. (5). We assume that the prey follows a radially symmetric reaction-diffusion process with homogeneous diffusion, and ignore reflecting boundary effects of the island, which is assumed to be a single point in space where the prey density is assumed to be zero. We then assume that the partial differential equation describing the dynamics of the density of prey $R(t,z)$ at time t is defined for all $z \in (0,\infty)$ according to

$$\frac{\partial R(t,z)}{\partial t} = \underbrace{\frac{m}{z}\frac{\partial}{\partial z}\left(z\frac{\partial R(t,z)}{\partial z}\right)}_{\text{diffusion}} - \underbrace{F(R(t,z),z,t)}_{\text{reaction}}. \tag{A7}$$

The first term on the right-hand side represents diffusion, occurring at rate m, to which we refer in the main text as movement rate. The second term represents reaction, which is some function of prey density, possibly distance from the island and time. Eq. (A7) corresponds to the two-dimensional reaction-diffusion process given by eq. (40) in Edelstein-Keshet (1988, Chapter 9).

But since the process is radially symmetric, it is written here in polar coordinates using eq. (61) in Edelstein-Keshet (1988, Chapter 9). The reaction term $F(R(t,z),z,t)$ is detailed below. Note that for a reaction term $F(z)$ that is independent of prey density and time, representing fixed consumption, eq. (A7) is equivalent to the consumption-dispersion model of Weber et al. (2021, their eq. 5).

At an equilibrium, $R(t,z) = R(z)$ and thus $\partial R(t,z)/\partial t = 0$ and $\partial^n R(t,z)/\partial z^n = \mathrm{d}^n R(z)/\,\mathrm{d}z^n$. Next, let us assume that the reaction term at such an equilibrium is given by

$$F(R(t,z),z,t) = g(R(z)) - \sum_{x\in\mathcal{X}} f(x,R(z),z)\frac{p(x,z)N(x)}{2\pi z}. \tag{A8}$$

The right-hand side is time-independent and the sum of a density-dependent prey growth rate $g(R(z))$ at distance z and the depletion rate $f(x,R(z),z)p(x,z)N(x)/(2\pi z)$ due to birds foraging at distance z, summed over all birds with trait values in $\mathcal{X} = \{x_1, x_2, \ldots, x_n\}$. Here, $p(x,z)N(x)/(2\pi z)$ is the density of individuals with trait value x at distance z, where the denominator $2\pi z$ accounts for the fact that individuals foraging at distance z distribute themselves randomly over the circumferences of the circle centered at the island. Hence, at equilibrium, eq. (A7) reduces to

$$0 = \underbrace{m\left(\frac{\mathrm{d}^2R(z)}{\mathrm{d}z^2} + \frac{1}{z}\frac{\mathrm{d}R(z)}{\mathrm{d}z}\right)}_{\text{diffusion}} + \underbrace{g(R(z)) - \sum_{x\in\mathcal{X}} f(x,R(z)z)\frac{p(x,z)N(x)}{2\pi z}}_{\text{reaction}}. \tag{A9}$$

Let us define

$$G(R(z),z) = g(R(z)) + m\left(\frac{\mathrm{d}^2R(z)}{\mathrm{d}z^2} + \frac{1}{z}\frac{\mathrm{d}R(z)}{\mathrm{d}z}\right) \tag{A10}$$

as the endogenous rate of change of prey density at distance z. Assuming that the bird community consists of only a single species ($\mathcal{X} = \{x\}$) so that the argument x can be dropped in all relevant functions, and substituting $G(R(z,z)$ into eq. (A10), we obtain eq. (5) in the main part.

In the absence of consumption, the last term on the right-hand side of eq. (A9) equals zero. We assume that the resulting equilibrium prey density is homogeneous over space and denote it as R^*. This satisfies eq. (A9) with $g(R^*) = 0$.

Appendix B The empirical foraging distributions and the single species ideal free distribution expressed as bird density

We here compare our single species ideal free distribution predicted from eqs. (12)–(13) to the empirical foraging distributions – when expressed as relative density – shown in fig. 2B in Weber et al. (2021). For our model, relative density $n(z)$ is proportional to the ideal free distribution $p(z)$ and given by

$$n(z) = \frac{p(z)N}{2\pi z}. \tag{B1}$$

The panels in the second row in figure B1 show how density $n(z)$ changes with distance z from the island for logistic and chemostat prey dynamics and different values of the search costs c_s. While fig. 2B of Weber et al. (2021) shows that density decreases monotonically with distance from the island, our model predicts a monotonic decline only under constant prey renewal ("chemostat dynamics") in combination with low values for the search costs c_s. To understand this, we note that from eqs. 12–13 we obtain

$$n(z) = \frac{B(R(z), z)G(R(z), z)}{\mu}. \tag{B2}$$

In the absence of search costs ($c_s = 0$), the net-energy content $B(R(z), z)$ of prey is decreasing with z due to increasing flight costs (see bottom row in fig. B1). However, this effect can easily be outweighed in the presence of search costs ($c_s \neq 0$) since the time spend searching ($T_s = 1/(aR(z))$) decreases with distance from the island due to the shape of the prey halo (gray hatched line in fig. 1a). The effect of the prey renewal rate $G(R(z), z)$ depends on the prey's growth rate $g(R(z))$. While for chemostat dynamics, prey growth is decreasing with increasing prey density (due to the prey depletion halo and the constant per-capita death rate, see equation for $g(R(z))$ in the legend of fig. 1), for logistic prey dynamics the prey growth rate is an unimodal function in z with a maximum at the distance where the prey density equilibrates at half its maximum density (third row in fig. B1).

We suggest that chemostat dynamics, describing the dynamics of a prey that is not self-renewable, might in fact be the better approximation for the prey dynamics investigated by Weber et al. (2021). The large-bodied seabirds subject of that study primarily feed on adult flying

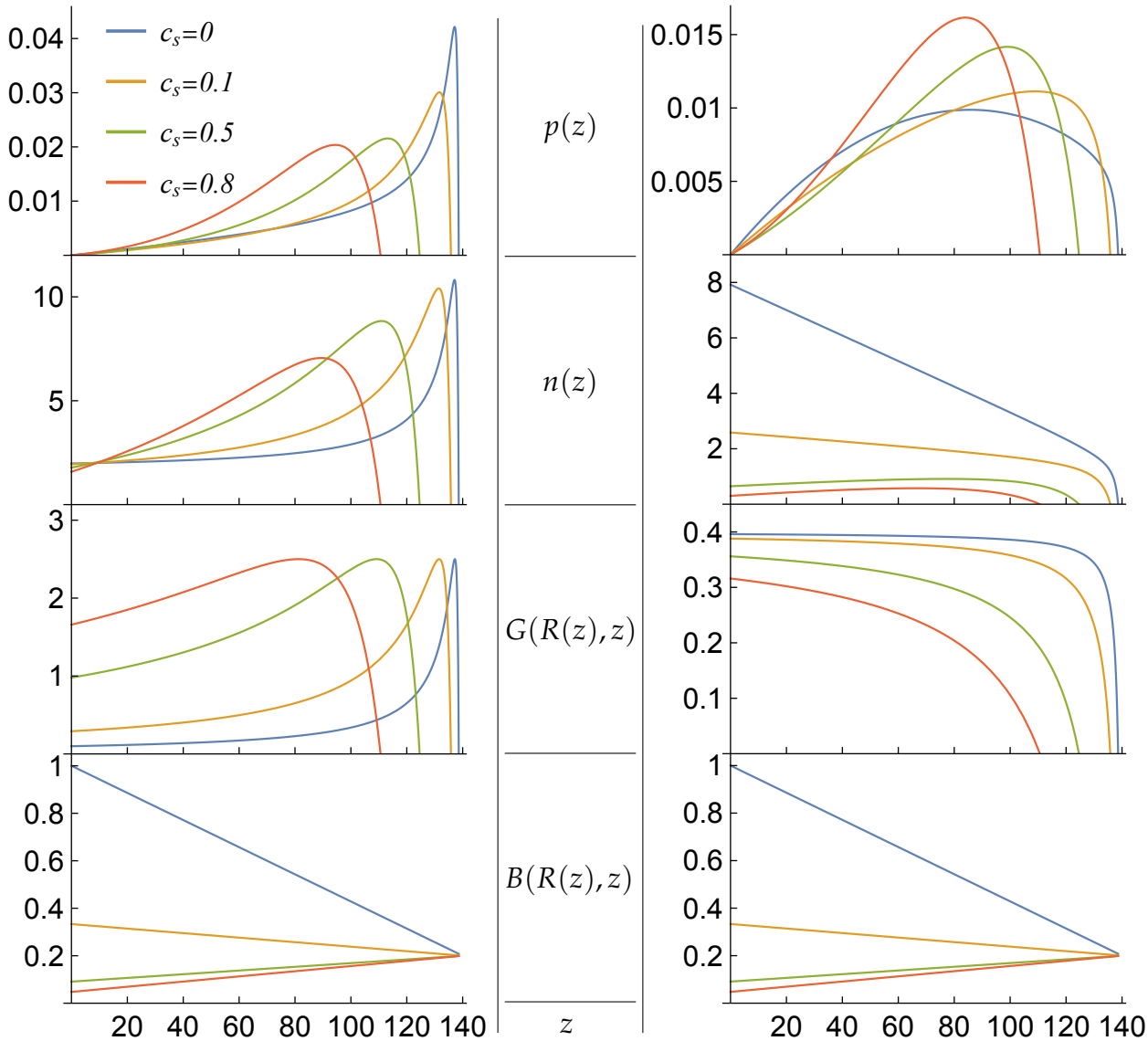

Figure B1: Ideal free distribution $p(z)$, bird density $n(z)$, prey renewal rate $G(R(z),z)$, and net energy content $B(R(z),z)$ at distance z for four different values of the search costs c_s under logistic (left side) and chemostat (right side) prey dynamics. Only for very low search costs c_s and chemostat prey dynamics is bird density monotonically declining with distance from the island. This is driven by a decreasing benefit with increasing distance due to increasing flight costs. For logistic prey dynamics, the bird density at distance z is largely driven by prey renewal $G(R(z),z)$ at that distance, which is always an unimodal function. Note, that $B(R(z),z)$ is independent of the type of prey dynamics. Parameters as in fig. 1(a), except for c_s, which is indicated by the color code, and $g(z)$ under chemostat dynamics, which is given by $g(R(z)) = b_R - d_R R(z)$ with $b_R = 0.4$ and $d_R = 0.0008$.

fish, and their renewal thus occurs through maturation of juvenile fish. We suggest that the constant renewal that is part of chemostat dynamics approximates this maturation, assuming that the juvenile fish stock is not strongly affected by the predation on adults. This might be approximately true given that intense bird predation occurs only during the breeding season, which lasts less than half a year. It is, however, noteworthy that in systems in which the dynamics of a self-renewing prey occurs on the same timescale as predation, the distribution of the consumers can be strongly shaped by the fact that prey can show the fastest renewal when they are far below their equilibrium. For logistic prey growth, the maximum growth rate occurs at half the equilibrium density. Based on eq. (11) and using the parameters from fig. B1, this occurs, with increasing values of c_s, at $z = 137.2, 131.6, 109.2, 92.4$. Given that fig. B1 is based on $m = 0$, this is where the curves for $G(R(z), z)$ peak and approximately where the curves for density $n(z)$ peak.

Appendix C Multi-species equilibrium and coexistence

In this appendix, we generalize the single species equilibrium conditions given by eqs. (11)–(13) to a community of interacting species.

Appendix C.1 Equilibrium conditions for prey, bird behavior and demography for n coexisting bird species

According to our assumptions, the equilibrium prey density $R(z)$, the ideal free distribution $p(x, z)$ of a species with trait value x, and the equilibrium abundance $N(x)$ of birds with that trait value in a community $\mathcal{X} = \{x_1, x_2, ..., x_n\}$ are determined by the following coupled system of equations, which generalizes the equilibrium of the single species model of the main text (section 2.2) to n species.

First, the prey at distance z at equilibrium balances renewal and consumption,

$$G(R(z), z) - \sum_{x \in \mathcal{X}} f(x, R(z), z) \frac{p(x, z) N(x)}{2\pi z} = 0. \tag{C1}$$

Here, the renewal function $G(R(z), z)$ is given by eq. (A10) while prey consumption is obtained from the assumption that the $N(x)$ birds of the species with trait value x are distributed according to the ideal free distribution $p(x, z)$, and that at distance z the $p(x, z)N(x)$ birds are

homogeneously distributed over the circumference of the circle centered at the island with radius z.

Second, the ideal free distribution $p(x,z)$ for each $x \in \mathcal{X}$ is characterized by the fact that the payoff obtained by individuals with trait value $x \in \mathcal{X}$ is identical at all distances where these individuals forage. Furthermore, the payoff at distances where individuals forage is at least as high as the payoff that would be obtained at distances where individuals do not forage. Thus, for each $x \in \mathcal{X}$ we have

$$\Pi(x,z) = \beta(x) \qquad \text{for all } z \in \mathbb{R}_+ \text{ with } p(x,z) > 0 \tag{C2a}$$

$$\Pi(x,z) \leq \beta(x) \qquad \text{for all } z \in \mathbb{R}_+ \text{ with } p(x,z) = 0. \tag{C2b}$$

Here, $\beta(x)$ is the constant payoff obtained at visited foraging distances to an individual with trait value x (the set of foraging distances satisfying eq. (C2a) is the support of the ideal free distribution). While the payoffs given by eq. (C2) do not depend explicitly on $p(x,z)$ (just as in the single species case), the dependence enters through eq. (C1) as the payoff depends on the equilibrium prey density $R(\mathcal{X},z)$, which depends on the ideal free distribution. At the ideal free distribution of the multispecies community characterized by eq. (C2), for each individual with trait value x and each $x \in \mathcal{X}$, we have

$$\Pi(x,y) \leq \Pi(x,z) \quad \text{for all } z \in \mathbb{R}_+ \text{ with } p(x,z) > 0 \text{ and all } y \in \mathbb{R}_+. \tag{C3}$$

This implies that no individual of any species has an incentive to unilaterally change behavior given all other individuals behave according to the ideal free distribution of their species. Thus, the multi-species ideal free distribution is a multi-species Nash equilibrium.

Third, the species with trait value $x \in \mathcal{X}$ is at its demographic equilibrium $N(x)$ when birth balances deaths,

$$\bar{\Pi}(x) = \mu. \tag{C4}$$

Here,

$$\bar{\Pi}(x) = \int_{z=0}^{z_{\max}(x)} p(x,z)\Pi(z)\,\mathrm{d}z \tag{C5}$$

is the mean payoff, which we equate to mean fecundity of an individual with trait value x.

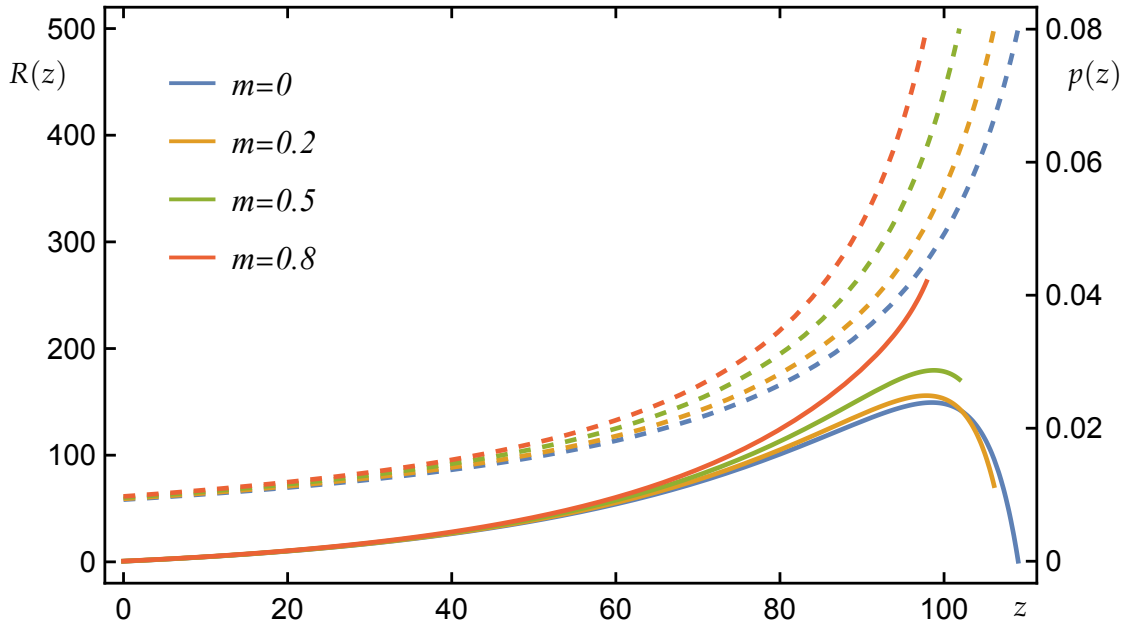

Figure C1: Equilibrium prey density $R(z)$ (hatched lines, left y-axis) and ideal free distribution $p(z)$ (solid lines, right y-axes) as function of distance z from the island for five different movement rates m and a fixed bird population size of 200000 individuals under logistic prey growth. In contrast to the results of bird populations at demographic equilibrium, as shown in fig. 1(a), the maximum flying distance decreases with increasing m and prey halos become less pronounced. Parameter values as in fig. 1.

Furthermore, $z_{\max}(x)$ is the maximum traveling distance of such an individual, as given by eq. (10). Here too, the dependence of the birth rate, given by average payoff, depends on $N(x)$ indirectly through the dependence of the equilibrium prey density on $N(x)$ (eq. C1).

The coupled system of equations (C1)-(C4) characterizes the prey equilibrium $R(z)$, the behavioral equilibrium $p(x,z)$ and the equilibrium bird abundance $N(x)$. We assume that this joint equilibrium exists and proceed to investigate it.

Appendix C.2 Properties of equilibrium prey densities

To determine the prey equilibrium and the behavioral and demographic equilibrium for multiple bird species, we start by presenting two properties of the equilibrium prey density distribution $R(x,z)$, which denotes the equilibrium prey density under the assumption that the population is monomorphic for trait value x (i.e., eq. 11).

First, for two species with trait values $x_1 \neq x_2$ the graphs of the equilibrium prey densities

$R(x_1, z)$ and $R(x_2, z)$ intersect at most once. To see this, set

$$R(x_1, z) = R(x_2, z), \tag{C6}$$

which, owing to eq. 11, is given by

$$\frac{\mu + c_\mathrm{s}(x_1)}{a(x_1)\left(b - \frac{2z}{v(x_1)}(c_\mathrm{f}(x_1) + \mu)\right)} = \frac{\mu + c_\mathrm{s}(x_2)}{a(x_2)\left(b - \frac{2z}{v(x_2)}(c_\mathrm{f}(x_2) + \mu)\right)}. \tag{C7}$$

This equality defines a linear equation in z, which can have at most one solution. The value of z satisfying the equality is the intersection point of the two equilibrium prey density distributions, which may lie beyond $z_\mathrm{max}(x_1)$ or $z_\mathrm{max}(x_2)$.

Second, $R(x, z)$ is convex in z in the interval $[0, z_\mathrm{max}(x))$. This can be seen from the second derivative of eq. (11) with respect to z, which is given by

$$\frac{\partial^2 R(x,z)}{\partial z^2} = \frac{2v(x)(\mu + c_\mathrm{f}(x))^2(\mu + c_\mathrm{s}(x))}{a(x)(bv(x) - z(\mu + c_\mathrm{f}(x)))^3}. \tag{C8}$$

The right-hand side is positive for $z < bv(x)/(\mu + c_\mathrm{f}(x))$. This is true for $z < z_\mathrm{max}$ as long as $z_\mathrm{max}(x) < bv(x)/(\mu + c_\mathrm{f}(x))$ holds, which is indeed the case as the following shows. By writing eq. (10) as

$$\begin{aligned} z_\mathrm{max}(x) =& \frac{v(x)\big(a(x)bR^* - \mu - c_\mathrm{s}(x)\big)}{2a(x)R^*(\mu + c_\mathrm{f}(x))} \\ =& \frac{bv(x)}{2(\mu + c_\mathrm{f}(x))}\left(1 - \frac{R(x,0)}{R^*}\right), \end{aligned} \tag{C9}$$

where

$$R(x, 0) = \frac{\mu + c_\mathrm{s}(x)}{a(x)b}. \tag{C10}$$

It follows that $z_\mathrm{max}(x) < bv(x)/(\mu + c_\mathrm{f}(x))$, because the term in parentheses on the right-hand side of eq. (C9) is less than 1. Thus, $\partial^2 R(x,z)/\partial z^2 > 0$ and the function $R(x, z)$ is convex in z for $z < z_\mathrm{max}(x)$.

Appendix C.3 Mutual exclusive foraging and prey depletion halo

We have now all concepts in place to determine the joint equilibrium conditions for prey, bird behavior and demography in a community of species with trait values $\mathcal{X}$. Let us first focus on two species, say species 1 with trait value x_1 and species 2 with trait value x_2. Assume that $R(x_1, 0) < R(x_2, 0)$ and $z_{\max}(x_1) < z_{\max}(x_2)$ (as an example, consider $x_1 = 3.5$ and $x_2 = 2$ with the parameters as in fig. C2). Then, given that the curves $R(x_1, z)$ and $R(x_2, z)$ are convex, the above ordering implies that they intersect exactly once, say, at the distance $z = z_1$. Given the assumption $R(x_1, 0) < R(x_2, 0)$, species 1 depletes prey to a lower density in the interval $[0, z_1]$ and thereby competitively excludes species 2. By contrast, species 2 depletes prey to a lower density in the interval $[z_1, z_{\max}(x_2)]$ and thereby competitively excludes species 1. In conclusion, the interval $[0, z_{\max}(x_2)]$ of utilized foraging distances can be partitioned into two mutually exclusive sub-intervals, such that $[0, z_{\max}(x_2)] = [0, z_1] \cup [z_1, z_{\max}(x_2)]$ and $z_1 = [0, z_1] \cap [z_1, z_{\max}(x_2)]$ (thus, with mutually exclusive we mean that two intervals intersect at most at their boundary). If, however, $R(x_1, 0) < R(x_2, 0)$ and $z_{\max}(x_1) > z_{\max}(x_2)$, then species 1 excludes species 2 over the whole interval $[0, z_{\max}(x_1)]$ of utilized foraging distances (as is the case for $x_1 = 0.5$ and $x_2 = 0.3$ in fig. C2). In summary, starting with a community $\mathcal{X} = \{x_1, x_2\}$, either the two species coexist by occupying two mutually exclusive distance intervals, or they mutually exclude each other with one species going extinct.

Suppose now that two species coexist and that we add a third species with trait value x_3 ($\mathcal{X} = \{x_1, x_2, x_3\}$) and that, in addition to the above ordering $R(x_1, 0) < R(x_2, 0)$ and $z_{\max}(x_1) < z_{\max}(x_2)$, we have, say, $R(x_2, 0) < R(x_3, 0)$ and $z_{\max}(x_2) < z_{\max}(x_3)$ (as an example, consider $x_1 = 3.5$, $x_2 = 2$ and $x_3 = 1$ with the parameters as in fig. C2). Since "is greater than" ($>$) is a transitive relation on the real numbers, we then also have $R(x_1, 0) < R(x_3, 0)$ and $z_{\max}(x_1) < z_{\max}(x_3)$. Due to the convexity of $R(x_1, z)$, $R(x_2, z)$ and $R(x_3, z)$, it follows that (i) the curves $R(x_2, z)$ and $R(x_3, z)$ intersect exactly once, say at z_2, and (ii) the intersection points z_1 (of $R(x_1, z)$ and $R(x_2, z)$) and z_2 have the ordering $z_1 < z_2$. Thus, the interval of utilized foraging distances can now be partitioned into three mutually exclusive distance intervals $[0, z_{\max}(x_3)] = [0, z_1] \cup [z_1, z_2] \cup [z_2, z_{\max}(x_3)]$. In each of these intervals, a different species induces the lowest equilibrium prey density. Hence, starting with a community $\mathcal{X} = \{x_1, x_2, x_3\}$, either the three species coexist by occupying three mutually exclusive bands (fig. C2 for $x_1 = 3.5$, $x_2 = 2$ and $x_3 = 1$), or two species coexist on

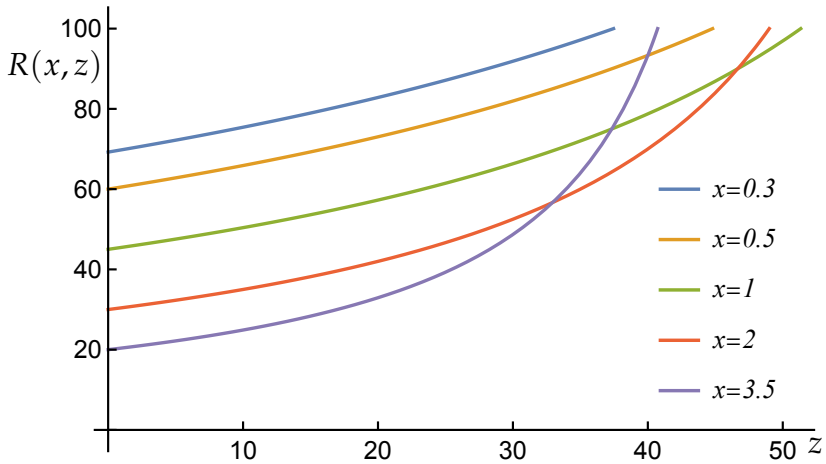

Figure C2: Equilibrium prey density $R(x,z)$ as a function of distance z for five different species, assuming that attack rate a and flying speed v are determined by the trait value x. This illustrates that, for certain parameters, not all equilibrium prey density curves intersect at z-values less than $z_{\max}$. The following sequence of community assembly could be envisaged. A community consisting of a species with $x = 0.3$ is replaced by an immigrant (or mutant) with $x = 0.5$, which in turn is replaced by a new species with $x = 1$. However, a further species with $x = 2$ does not replace the species with $x = 1$ but coexist with it (where the species with $x = 1$ is restricted to a small interval at a large distance from the island. Upon the arrival of a species with $x = 3.5$, a community of three coexisting species has emerged. Parameter values as in fig. 1(a) except for $\alpha = 0.001$. As a result, $R^* = 100$, which makes condition (D9), specifying when a trade-off between v and a results in a trade-off between $R(x,0)$ and $z_{\max}(x)$, more restrictive.

mutually exclusive bands (fig. C2 for $x_1 = 3.5$, $x_2 = 2$ and $x_3 = 0.5$), or only one species persists (fig. C2 for $x_1 = 1$, $x_2 = 0.5$ and $x_3 = 0.3$).

By induction, this argument generalizes to a community $\mathcal{X} = \{x_1, x_2, ..., x_n\}$. Suppose, the ordering of the maximum flying distances of the n species, say, $z_{\max}(x_1) < z_{\max}(x_2) < ... < z_{\max}(x_n)$ matches the ordering of their equilibrium prey distribution at distance $z = 0$, $R(x_1, 0) < R(x_2, 0) < ... < R(x_n, 0)$ (i.e., larger maximum flying distance implies a higher equilibrium prey density at distance $z = 0$). Then, the interval $(0, z_{\max}(x_n))$ of utilized foraging distances can be partitioned into the n distance intervals $[0, z_1]$, $[z_{i-1}, z_i]$ for $i \in \{2, \ldots, n-1\}$ and $[z_{n-1}, z_{\max}(n)]$, where z_i ($i \in \{1, \ldots, n\}$) is obtained by solving the linear equation $R(x_i, z_i) = R(x_{i+1}, z_i)$. These intervals fulfill

$$[0, z_{\max}(x_n)] = [0, z_1] \cup [z_1, z_2] \cup ... \cup [z_{n-1}, z_{\max}(x_n)] \tag{C11}$$

and any two intervals intersect at most at a common boundary. Thus, they are mutually exclusive.

Each interval is occupied by the species that depletes prey to the lowest equilibrium density in that interval, and the equilibrium prey distribution equals

$$R(z) = \begin{cases} 0 & \text{for } z = 0 \\ R(x_i, z) & \text{for } i \in \{1, \ldots, n\} \text{ and } z_{i-1} < z \leq z_i \\ R^* & \text{for } z > z_{\max}(x_n). \end{cases} \tag{C12}$$

where we set $z_{i-1} = 0$ for $i = 1$ and $z_i = z_{\max}(x_n)$ for $i = n$. The behavioral strategy equals

$$p(x_i, z) = \begin{cases} \dfrac{2\pi z}{N(x_i)} \dfrac{G(R(x_i, z), z)}{f(x_i, R(x_i, z), z)} & \text{for } i \in \{1, \ldots, n\} \text{ and } z_{i-1} \leq z \leq z_i \\ 0 & \text{for } z > z_{\max}(x_n) \end{cases} \tag{C13}$$

where

$$N(x_i) = \frac{2\pi}{\mu} \int_{z_{i-1}}^{z_i} z\Big(b - c_{\mathrm{f}}(x_i) T_{\mathrm{f}}(x_i, z) - c_{\mathrm{s}}(x_i) T_{\mathrm{s}}(x_i, z)\Big) G(R(x_i, z), z) \, \mathrm{d}z \tag{C14}$$

denotes the equilibrium population size of species i (compare eq. 13). Eqs. (C12) and (C13) provide an equilibrium prey distribution and ideal free distribution (satisfying $\int_{z_{i-1}}^{z_i} p(x_i, z) \, \mathrm{d}z = 1$), since the system of equations (C1)-(C2) is satisfied. Together, eqs. (C12)-(C14) provide an explicit representation of the joint equilibrium for prey, bird behavior and demography for n coexisting bird species. The salient feature is that a single bird species occupies a given interval, and no two species can coexist within the same interval.

Appendix D Trade-offs

Each species is characterized by a quantitative trait value $x \in \mathbb{R}$ that determines the value of the four foraging components $a(x)$, $v(x)$, $c_{\mathrm{f}}(x)$ and $c_{\mathrm{s}}(x)$. In Appendix C.3, we established that for two species with trait values x_1 and x_2 to be able to coexist due to behavioral niche partitioning, it is necessary and sufficient that the graphs of the equilibrium prey densities – induced by each species in isolation – intersect at some distance z that lies within the maximum flying distance of both species. This is the case if and only if $R(x_1, 0) < R(x_2, 0)$ and $z_{\max}(x_1) < z_{\max}(x_2)$ (or vice versa). In other words, the species that depletes the prey to a lower equilibrium density close to the island also has a lower maximum flying distance. This can be interpreted as a trade-off

between a species' ability to use prey efficiently in the absence of travel costs (close to the island) and in the presence of significant travel costs (resulting in a higher maximum travel distance). In this appendix, we investigate for which pairs of foraging components such a trade-off emerges, which is what we present in table 1 in the main part. We do this in two steps. First, in Appendix D.1 we establish how each foraging component affects $R(x_1, 0)$ and $z_{\max}(x)$. Second, in Appendix D.2 we ask how changing the trait value x affects $R(x_1, 0)$ and $z_{\max}(x)$. To answer this second questions, we make use of the results from the first step. Assuming that more than two foraging components depend on x does not lead to qualitatively new results.

Appendix D.1 Effects of foraging components on the prey depletion halo

From eqs. (10)–(11) we see that two characteristics of the prey depletion halo, $R(x, 0)$ and $z_{\max}(x)$, can be written explicitly in terms of trait values as

$$R(x,0) = \frac{\mu + c_{\mathrm{s}}(x)}{a(x)(b(x)} \quad \text{and} \quad z_{\max} = \frac{v\big(a(x)bR^* - \mu - c_{\mathrm{s}}(x)\big)}{2a(x)R^*(\mu + c_{\mathrm{f}}(x))}. \tag{D1}$$

The derivatives of these two quantities with respect to capture efficiency are

$$\frac{\mathrm{d}R(x,0)}{\mathrm{d}a(x)} = -\frac{c_{\mathrm{s}}(x) + \mu}{ba(x)^2} < 0 \tag{D2a}$$

$$\frac{\mathrm{d}z_{\max}}{\mathrm{d}a(x)} = \frac{v(x)(c_{\mathrm{s}}(x) + \mu)}{R^* a(x)^2 (c_{\mathrm{f}}(x) + \mu)} > 0. \tag{D2b}$$

Thus, increasing $a(x)$ lowers the prey equilibrium curve $R(x, z)$ at all distances z.

The derivatives with respect to flying speed are

$$\frac{\mathrm{d}R(x,0)}{\mathrm{d}v(x)} = 0 \tag{D3a}$$

$$\frac{\mathrm{d}z_{\max}}{\mathrm{d}v(x)} = \frac{bR^* a(x) - c_{\mathrm{s}}(x) - \mu}{R^* a(x)(c_{\mathrm{f}}(x) + \mu)} > 0. \tag{D3b}$$

From eqs. (1)-(3) follows that the numerator on the right-hand side of eq. (D3b) can be interpreted as the per-capita growth rate of a species foraging at $z = 0$ and in the absence of competition such that the prey density is given by R^*. For a population to be able to persist, this quantity has to be positive. Thus, increasing $v(x)$ lowers the equilibrium prey density curve $R(x, z)$ at all

distances $z > 0$.

The derivatives with respect to flying cost are

$$\frac{\mathrm{d}R(x,0)}{\mathrm{d}c_{\mathrm{f}}(x)} = 0 \tag{D4a}$$

$$\frac{\mathrm{d}z_{\max}}{\mathrm{d}c_{\mathrm{f}}(x)} = -\frac{v(x)(bR^{*}a(x) - c_{\mathrm{s}}(x) - \mu)}{R^{*}a(x)(c_{\mathrm{f}}(x) + \mu)^{2}} < 0. \tag{D4b}$$

Thus, increasing $c_{\mathrm{f}}(x)$ raises the equilibrium prey density curve $R(x,z)$ at all distances $z > 0$.

Finally, the derivatives with respect to search cost are

$$\frac{\mathrm{d}R(x,0)}{\mathrm{d}c_{\mathrm{s}}(x)} = \frac{1}{ba(x))} > 0 \tag{D5a}$$

$$\frac{\mathrm{d}z_{\max}}{\mathrm{d}c_{\mathrm{s}}(x)} = -\frac{v(x)}{R^{*}a(x)(c_{\mathrm{f}}(x) + \mu)} < 0. \tag{D5b}$$

Thus, increasing $c_{\mathrm{f}}(x)$ raises the equilibrium prey density curve $R(x,z)$ at all distances z.

Appendix D.2 Trade-off pairs

In the following calculations, we omit the argument x from any foraging component that is not assumed to depend on x. Primes denote derivatives with respect to x.

For the quantitative trait x to have the potential to impose a trade-off between $R(0,x)$ and $z_{\max}(x)$, we assume that x maps to the considered foraging components such that the effect of increasing x decreases $R(0,x)$ and $z_{\max}(x)$ through one foraging component and increases $R(0,x)$ and $z_{\max}(x)$ through the other foraging component. Changing x indeed induces a trade-off if an increase in x decreases $R(0,x)$ and $z_{\max}(x)$ (increased competitiveness close to the island at the cost of decreased competitiveness far way from the island), or vice versa.

Trade-off between $a(x)$ and $v(x)$. Based on eqs. (D2) and (D3), to impose a trade-off we assume

$$a'(x) > 0 \quad \text{and} \quad v'(x) < 0. \tag{D6}$$

For the derivatives, we find

$$\frac{\mathrm{d}R(x,0)}{\mathrm{d}x} = -\frac{a'(x)(c_\mathrm{s}+\mu)}{ba(x)^2} < 0, \tag{D7a}$$

$$\frac{\mathrm{d}z_\mathrm{max}(x)}{\mathrm{d}x} = \frac{a'(x)v(x)(c_\mathrm{s}+\mu) + a(x)v'(x)(bR^*a(x) - c_\mathrm{s} - \mu)}{R^*a(x)^2(c_\mathrm{f}+\mu)}. \tag{D7b}$$

For a trade-off to exist, the right-hand side of eq. (D7b) has to be negative. This is equivalent to

$$-\frac{a'(x)}{v'(x)}\frac{v(x)}{a(x)} > \frac{bR^*a(x) - c_\mathrm{s} - \mu}{c_\mathrm{s}+\mu}. \tag{D8}$$

Due to eq. (D6), the function $v(x)$ and is invertible and differentiable with derivative $1/v'(x)$. With this, we can rewrite the last inequality as

$$-\frac{\mathrm{d}a(x)}{\mathrm{d}v(x)}\frac{v(x)}{a(x)} > \frac{bR^*a(x) - c_\mathrm{s} - \mu}{c_\mathrm{s}+\mu}. \tag{D9}$$

The left-hand side of this inequality gives the slope of the parametric curve that plots $a(x)$ and $v(x)$ as a function of x, to which we refer as trade-off curve, weighted by the inverse ratio of the two foraging components. Note, that, due to (D6), this trade-off curve has a negative slope. The left-hand side of inequality(D9) is known as the elasticity of the trade-off curve (the percentage change in $a(x)$ with percentage change in $v(x)$; e.g., Sydsæter and Hammond, 1995, p. 171-4).

Trade-off between $a(x)$ and $c_\mathrm{f}(x)$. Based on eqs. (D2) and (D4), to impose a trade-off we assume

$$a'(x) > 0 \quad \text{and} \quad c_\mathrm{f}'(x) > 0. \tag{D10}$$

For the derivatives we find

$$\frac{\partial R(x,0)}{\partial x} = -\frac{a'(x)(c_\mathrm{s}+\mu)}{ba(x)^2} < 0, \tag{D11a}$$

$$\frac{\mathrm{d}z_\mathrm{max}(x)}{\mathrm{d}x} = \frac{v\big(a'(x)(c_\mathrm{s}+\mu)(c_\mathrm{f}(x)+\mu) - a(x)c_\mathrm{f}'(x)(bR^*a(x) - c_\mathrm{s} - \mu)\big)}{R^*a(x)^2(c_\mathrm{f}(x)+\mu)}. \tag{D11b}$$

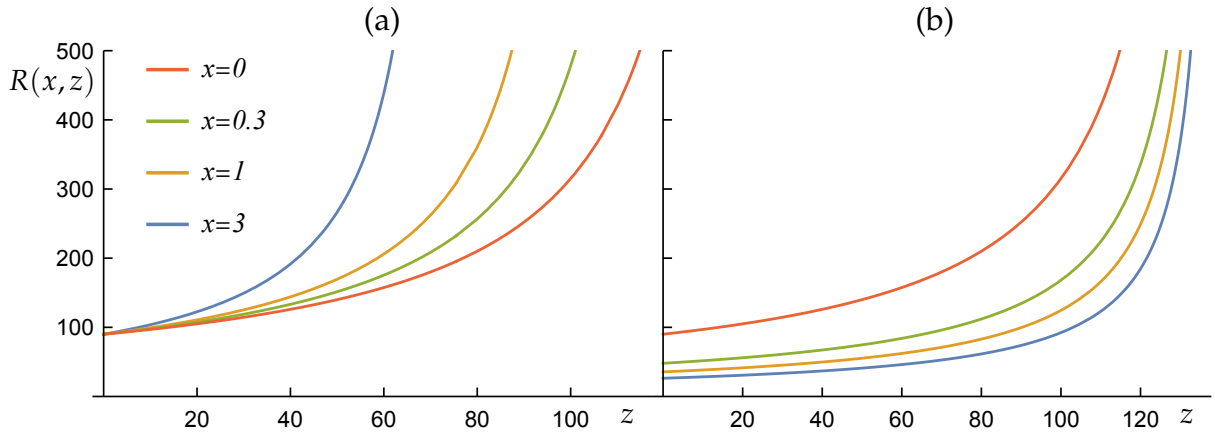

Figure D1: Equilibrium prey density $R(x,z)$ as a function of distance z for four different trait values x, assuming that (a) flying speed $v(x)$ and flying costs $c_\mathrm{f}(x)$ and (b) attack rate $a(x)$ and search costs $c_\mathrm{s}(x)$ are trait-dependent. In the first case, all equilibrium prey density curves intersect at $z = 0$ while they never intersect in the second case. In both cases, coexistence of different species is impossible and the species with the lowest equilibrium prey density curve excludes all others ($x = 0$ in (a) and $x = 10$ in (b)). The functions $a(x)$ and $v(x)$ are as described in the legend of fig. 2. For flying and search costs, we use $c_\mathrm{f}(x) = c_{\mathrm{f}0}/(1 + c_{\mathrm{f}1}x)$ and $c_\mathrm{s}(x) = c_{\mathrm{s}0}/(1 + c_{\mathrm{s}1}x)$, respectively, with parameters $c_{\mathrm{f}0} = 0.2$, $c_\mathrm{fb} = 0.01$, $c_{\mathrm{s}0} = 0.4$ and $c_{\mathrm{s}1} = 0.1$. Other parameter values as in fig. 1(a).

For a trade-off to exist, the right-hand side of eq. (D11b) has to be negative. Factoring out $a'(x)/c_\mathrm{f}'(x) = \mathrm{d}a(x)/\,\mathrm{d}c_\mathrm{f}(x)$, this is equivalent to

$$\frac{bR^*a(x) - c_\mathrm{s}(x) - \mu}{c_\mathrm{s}(x) + \mu} > \frac{\mathrm{d}a(x)}{\mathrm{d}c_\mathrm{f}(x)}\frac{c_\mathrm{f}(x) + \mu}{a(x)}. \tag{D12}$$

Trade-off between $a(x)$ and $c_\mathrm{s}(x)$. In this case, solving eq. (C7) for z shows that different equilibrium prey density functions do not intersect with each other (as in fig. D1b). Thus, for a given set of species $\mathcal{X}$, the species x corresponding to the lowest equilibrium prey density curve excludes all other species and coexistence is impossible.

Trade-off between $v(x)$ and $c_\mathrm{f}(x)$. In this case, solving eq. (C7) for z shows that different equilibrium prey density functions always intersect with each other at $z = 0$ (as in fig. D1a). Thus, for a given set of species $\mathcal{X}$, the species x corresponding to the lowest equilibrium prey density curve excludes all other species and coexistence is impossible.

Trade-off between $v(x)$ and $c_s(x)$. Based on eqs. (D2) and (D5), to impose a trade-off we assume

$$a'(x) > 0 \quad \text{and} \quad c_s'(x) > 0. \tag{D13}$$

For the derivatives we find

$$\frac{\partial R(x,0)}{\partial x} = \frac{c_s'(x)}{ba} > 0, \tag{D14a}$$

$$\frac{\mathrm{d}z_{\max}(x)}{\mathrm{d}x} = \frac{v'(x)(bR^*a - c_s(x) - \mu) - v(x)c_s'(x)}{aR^*(c_f + \mu)}. \tag{D14b}$$

For a trade-off to exist, the right-hand side of eq. (D14b) has to be positive. Factoring out $v'(x)/c_s'(x) = \mathrm{d}v(x)/\,\mathrm{d}c_s(x)$, this is equivalent to

$$\frac{\mathrm{d}v(x)}{\mathrm{d}c_s(x)} \frac{bR^*a - c_s(x) - \mu}{v(x)} > 1. \tag{D15}$$

Trade-off between $c_f(x)$ and $c_s(x)$. Based on eqs. (D4) and (D5), to impose a trade-off we assume

$$c_f'(x) > 0 \quad \text{and} \quad c_s'(x) < 0. \tag{D16}$$

For the derivatives we find

$$\frac{\partial R(x,0)}{\partial x} = \frac{c_s'(x)}{ba} > 0, \tag{D17a}$$

$$\frac{\mathrm{d}z_{\max}(x)}{\mathrm{d}x} = -\frac{v\big(c_f'(x)(bR^*a - c_s(x) - \mu) + c_s'(x)(c_f(x) + \mu)\big)}{aR^*(\mu + c_f(x))^2}. \tag{D17b}$$

A trade-off exists if eq. (D17b) is positive. Factoring out $c_f'(x)/c_s'(x) = \mathrm{d}c_f(x)/\,\mathrm{d}c_s(x)$, this is equivalent to

$$-\frac{\mathrm{d}c_f(x)}{\mathrm{d}c_s(x)} \frac{bR^*a - c_s(x) - \mu}{c_f(x) + \mu} > 1. \tag{D18}$$

Appendix E Group foraging

We here derive the model of group foraging described in Box 1. Thus, we keep all assumptions of the foraging process the same as under the model for individual foraging, except that (i) all individuals express an identical foraging behavior, (ii) population (group) size N is fixed, and

(iii) prey individuals cannot migrate ($m = 0$). Since we consider groups consisting of a single species, we henceforth omit the argument x from all variables.

From the model of individual foraging we know that a maximal foraging distance $z_{\max}$ exists beyond which payoff is negative and distances beyond this point will never be visited in any behavioral equilibrium. Accordingly, we can write the expected payoff to an individual with behavioral strategy $p : [0, z_{\max}] \to R_+$ under group foraging as

$$\bar{\Pi}(z_{\max}, p) = \int_0^{z_{\max}} p(z)\Pi(z)\,\mathrm{d}z \tag{E1}$$

subject to the constraint that

$$\int_0^{z_{\max}} p(z)\,\mathrm{d}z = 1, \tag{E2}$$

and where

$$\Pi(z) = f(R(z), z)B(R(z), z) \tag{E3}$$

is the payoff from foraging at distance z. Eq. (E1) is the net rate of energy uptake to an individual under group foraging and can equivalently be interpreted as the foraging group's average per-capita energy uptake. Here, $B(R(z), z)$ and $f(R(z), z)$ are defined as in eqs. (1) and (2). Furthermore, analogous to eq. (5) in the absence of movement ($m = 0$), the equilibrium prey density $R(z)$ at distance z satisfies

$$g(R(z)) = f(R(z), z)\frac{p(z)N}{2\pi z}. \tag{E4}$$

Thus, the mean payoff defined by eq. (E1) is equivalent to that defined by eq. (4).

The behavior p in eqs. (E1) and (E4), however, does not yet represent an equilibrium. To find the equilibrium, we have to maximize the payoff $\bar{\Pi}(p)$ with respect to p and the maximum foraging distance $z_{\max}$ under the integral constraints given by (E2). To solve this optimization problem, we follow standard optimization techniques using calculus of variations (e.g. Bryson and Ho, 1975; Sydsæter et al., 2008). We note that our problem is equivalent to an optimal control problem with a free boundary point and an integral constraint (e.g., Bryson and Ho, 1975, section 2.8 and 3.1). Accordingly, we construct the Lagrangian function

$$L(p, z_{\max}) = \int_0^{z_{\max}} p(z)\Pi(z)\,\mathrm{d}z - \lambda\left(\int_0^{z_{\max}} p(z)\,\mathrm{d}z - 1\right), \tag{E5}$$

where λ is the Lagrange multiplier associated to the integral constraint. The necessary first-order conditions for the function p and the distance $z_{\max}$ to maximize payoff are

$$\frac{\partial L(p, z_{\max})}{\partial p(z)} = \Pi(z) + p(z)\frac{\partial \Pi(z)}{\partial R(z)}\frac{\partial R(z)}{\partial p(z)} - \lambda = 0 \quad \text{for all } z \in [0, z_{\max}] \tag{E6a}$$

$$\frac{\partial L(p, z_{\max})}{\partial z_{\max}} = \Pi(z_{\max}) - \lambda = 0 \tag{E6b}$$

(a special case of Bryson and Ho, 1975, eqs. 2.8.17 and 2.8.20 with a Lagrangian function given by their eq. 3.1.4). Note, that for simplicity of presentation, in the second term on the right-hand side of eq. (E6a) we omit writing the functions explicitly in terms of the arguments with respect to which partial derivatives are taken. The first term in this derivative, $\Pi(z)$, describes the payoff gain to an individual from increasing its tendency to forage at distance z and is thus a benefit. The second term describes the change in payoff that results from increased prey depletion at a distance z that comes with an increased tendency to forage at that distance. The Lagrange multiplier λ can be interpreted as the payoff that is lost at equilibrium if the constraint could be loosened infinitesimally (e.g., Sydsæter et al., 2008). Eq. (E6a) says that the gain from foraging at distance z must be balanced by the cost of increasing competition from foraging at z and the cost this entails. Finally, note that by comparing eq. (E6b) and eq. (E5) it follows that $p(z_{\max}) = 0$.

Eqs. (E6a)–(E6b) show that a candidate equilibrium density $p(z)$ at z has to satisfy

$$p(z) = F(p(z), \lambda, z) \tag{E7}$$

with

$$F(p(z), \lambda, z) = \frac{\lambda - \Pi(z)}{\frac{\partial \Pi(z)}{\partial R(z)}\frac{\partial R(z)}{\partial p(z)}}, \tag{E8}$$

where

$$\frac{\partial \Pi(z)}{\partial R(z)} = \frac{a\left(b + (c_{\mathrm{s}} - c_{\mathrm{f}})T_{\mathrm{f}}(z)\right)}{\left(1 + aT_{\mathrm{f}}(z)R(z)\right)^2}, \tag{E9a}$$

$$\frac{\partial R(z)}{\partial p(z)} = \frac{Nf(z)}{2\pi z\frac{\mathrm{d}g(R(z))}{\mathrm{d}R(z)} - Np(z)\frac{\partial f(z)}{\partial R(z)}}. \tag{E9b}$$

The last equality is obtained by implicit differentiation of eq. (E4) and where $\partial f(z)/\partial R(z)$ de-

pends on $p(z)$ owing to eq. (E4). The argument $p(z)$ in $F(p(z), \lambda, z)$ emphasizes that the density $p(z)$ in eq. (E7) is defined only implicitly. But this density can be solved by finding the solution $p(z)$ satisfying eq. (E7) if λ is known, which in turn can be obtained by solving

$$\int_0^{z_{\max}} F(p(z), \lambda, z)\, \mathrm{d}z = 0 \qquad \text{and} \qquad \Pi(z_{\max}) = \lambda \tag{E10}$$

for λ and $z_{\max}$.

In conclusion, once the nature of the prey's growth rate $g(R(z))$ is specified, the system of equations given by eqs. (E7)–(E10) in combination with eqs. (E3)–(E4) allows us to compute the candidate behavioral equilibrium $(p, z_{\max})$, consisting of a foraging distribution and a maximal foraging distance, fulfilling eq. (E7). To ascertain that this is indeed a maximum, one would need to evaluate second-order or sufficiency conditions for a local or global maximum. The literature on control theory does not provide any simple recipe to check any such conditions in the context of free boundary point optimal control problems (e.g., Seierstad and Sydsæter, 1987, Theorem 13, p. 145), and our problem is furthermore compounded with an integral constraint. Hence, we argue somewhat heuristically that the equilibria identified numerically in fig. 3 are indeed maxima. For this, we note that, because there is no prey at $z = 0$ and because payoff decrease with distance z in an environment without competitors, the optimal solution has to be a function $p : [0, z_{\max}] \to R_+$ with $z_{\max} > 0$ and $p(z) > 0$ for all $z \in (0, z_{\max}]$. Second, in the numerical analysis underlying fig. 3, we find a single positive solution $p(z)$ for each $z \in (0, z_{\max}]$ satisfying eq. (E7). This thus has to characterize a maximum.